Regulatory variants in *TCF7L2* are associated with thoracic aortic aneurysm

Tanmoy Roychowdhury,[1,27] Haocheng Lu,[1,27] Whitney E. Hornsby,[1] Bradley Crone,[2] Gao T. Wang,[3] Dong-chuan Guo,[4] Anoop K. Sendamarai,[5,6,7] Poornima Devineni,[5] Maoxuan Lin,[1,8] Wei Zhou,[1,9,10] Sarah E. Graham,[1] Brooke N. Wolford,[2] Ida Surakka,[1] Zhenguo Wang,[1] Lin Chang,[1] Jifeng Zhang,[1] Michael Mathis,[2,11] Chad M. Brummett,[11] Tori L. Melendez,[1] Michael J. Shea,[1] Karen Meekyong Kim,[12] G. Michael Deeb,[12] Himanshu J. Patel,[12] Jonathan Eliason,[13] Kim A. Eagle,[1] Bo Yang,[12] Santhi K. Ganesh,[1,14] Ben Brumpton,[15,16,17] Bjørn Olav Åsvold,[15,17,18] Anne Heidi Skogholt,[15] Kristian Hveem,[15,17] VA Million Veteran Program, Saiju Pyarajan,[5,7] Derek Klarin,[19,20,21] Philip S. Tsao,[22,23] Scott M. Damrauer,[24,25] Suzanne M. Leal,[3,26] Dianna M. Milewicz,[4] Y. Eugene Chen,[1,12] Minerva T. Garcia-Barrio,[1,*] and Cristen J. Willer[1,2,14,*]

Summary

Thoracic aortic aneurysm (TAA) is characterized by dilation of the aortic root or ascending/descending aorta. TAA is a heritable disease that can be potentially life threatening. While 10%–20% of TAA cases are caused by rare, pathogenic variants in single genes, the origin of the majority of TAA cases remains unknown. A previous study implicated common variants in *FBN1* with TAA disease risk. Here, we report a genome-wide scan of 1,351 TAA-affected individuals and 18,295 control individuals from the Cardiovascular Health Improvement Project and Michigan Genomics Initiative at the University of Michigan. We identified a genome-wide significant association with TAA for variants within the third intron of *TCF7L2* following replication with meta-analysis of four additional independent cohorts. Common variants in this locus are the strongest known genetic risk factor for type 2 diabetes. Although evidence indicates the presence of different causal variants for TAA and type 2 diabetes at this locus, we observed an opposite direction of effect. The genetic association for TAA colocalizes with an aortic eQTL of *TCF7L2*, suggesting a functional relationship. These analyses predict an association of higher expression of *TCF7L2* with TAA disease risk. *In vitro*, we show that upregulation of *TCF7L2* is associated with *BCL2* repression promoting vascular smooth muscle cell apoptosis, a key driver of TAA disease.

Introduction

Thoracic aortic aneurysm (TAA) is characterized by dilation of the aortic root, ascending aorta, the aortic arch, and descending aorta. TAA often develops asymptomatically over a period of time, and thus, early diagnosis of TAA is quite challenging. Aneurysms in thoracic aorta are frequently followed by rupture or dissection of aortic tissue, which can be fatal. Early diagnosis through selective screening of individuals with the highest genetic risk of TAA can potentially reduce the risk of death through early surgical intervention.[1]

Approximately 10%–20% of TAA cases are monogenic, i.e., due to rare, pathogenic variants in single genes.[2,3] Variants in at least 11 such genes (*ACTA2*, *COL3A1*, *FBN1*, *MYH11*, *SMAD3*, *TGFB2*, *TGFBR1*, *TGFBR2*, *MYLK*, *LOX*, and *PRKG1*) are associated with strong risk of TAA[4] and were primarily identified through family studies. Monogenic TAAs are often present with syndromic heritable thoracic aortic disorders, including Marfan, Loeys-Dietz,

[1]Department of Internal Medicine, Division of Cardiovascular Medicine, University of Michigan, Ann Arbor, MI 48109, USA; [2]Department of Computational Medicine and Bioinformatics, University of Michigan, Ann Arbor, MI 48109, USA; [3]Center for Statistical Genetics, Gertrude H. Sergievsky Center, and the Department of Neurology, Columbia University Medical Center, New York, NY 10032, USA; [4]Department of Internal Medicine, McGovern Medical School, University of Texas Health Science Center at Houston, Houston, TX 70030, USA; [5]Center for Data and Computational Sciences, VA Boston Healthcare System, Boston, MA 02130, USA; [6]Booz Allen Hamilton, McLean, VA 22102, USA; [7]Department of Medicine, Harvard Medical School, Boston, MA 02115, USA; [8]Department of Otolaryngology–Head and Neck Surgery, Massachusetts Eye and Ear, Boston, MA 02114, USA; [9]Analytic and Translational Genetics Unit, Massachusetts General Hospital, Boston, MA 02114, USA; [10]Stanley Center for Psychiatric Research, Broad Institute of Harvard and MIT, Cambridge, MA 02142, USA; [11]Department of Anesthesiology, University of Michigan, Ann Arbor, MI 48109, USA; [12]Department of Cardiac Surgery, University of Michigan, Ann Arbor, MI 48109, USA; [13]Department of Surgery, Section of Vascular Surgery, University of Michigan, Ann Arbor, MI 48109, USA; [14]Department of Human Genetics, University of Michigan, Ann Arbor, MI 48109, USA; [15]K.G. Jebsen Center for Genetic Epidemiology, Department of Public Health and Nursing, NTNU, Norwegian University of Science and Technology, Trondheim 7030, Norway; [16]Clinic of Medicine, St. Olavs Hospital, Trondheim University Hospital, Trondheim 7030, Norway; [17]HUNT Research Center, Department of Public Health and Nursing, NTNU, Norwegian University of Science and Technology, Levanger 7600, Norway; [18]Department of Endocrinology, Clinic of Medicine, St. Olavs Hospital, Trondheim University Hospital, Trondheim 7030, Norway; [19]Malcolm Randall VA Medical Center, Gainesville, FL 32608, USA; [20]Division of Vascular Surgery and Endovascular Therapy, University of Florida College of Medicine, Gainesville, FL 32608, USA; [21]Program in Medical and Population Genetics, Broad Institute of MIT and Harvard, Cambridge, MA 02142, USA; [22]VA Palo Alto Health Care System, Palo Alto, CA 94304, USA; [23]Division of Cardiovascular Medicine, Stanford University School of Medicine, Stanford, CA 94305-5406, USA; [24]Department of Surgery, Corporal Michael Crescenz VA Medical Center, Philadelphia, PA 19104, USA; [25]Department of Surgery, Perelman School of Medicine, University of Pennsylvania, Philadelphia, PA 19104, USA; [26]Taub Institute for Alzheimer disease and the Aging Brain, Columbia University, NY 10032, USA
[27]These authors contributed equally
*Correspondence: cristen@umich.edu (C.J.W.), minerva@med.umich.edu (M.T.G.-B.)
https://doi.org/10.1016/j.ajhg.2021.06.016.

Ehlers-Danlos, and smooth muscle dysfunction syndromes.[5,6] Moreover, approximately 50% of individuals with congenital heart malformations, such as bicuspid aortic valve (BAV), later develop TAA.[7] Yet the origin of the majority of TAA cases remains unknown. It is likely that these cases have more complex origins, involving common genetic variants affecting many genes. Genome-wide association studies (GWASs) have been particularly successful in identifying common genetic variants that increase disease risk. Previously, common variants in *FBN1* were found to be associated with TAA.[8] Another study implicated *LRP1* and *ULK4* in acute thoracic aortic dissection.[9]

In an attempt to identify genetic associations with TAA, we performed a GWAS of 1,351 TAA-affected individuals and 18,295 control individuals and identified a previously unpublished genome-wide significant locus in the third intron of *TCF7L2*. We replicated this signal with meta-analysis of four additional independent cohorts. At this locus, an inverse association between TAA and type 2 diabetes (T2D) was observed. The association signal colocalizes with an eQTL of *TCF7L2* in aorta, providing functional insight into the genetic association. *In vitro*, we show a potential role of *TCF7L2* in vascular smooth muscle cell (VSMC) apoptosis, a key TAA disease mechanism.

Material and methods

Description of the discovery cohorts

The Cardiovascular Health Improvement Project (CHIP) is a cohort with genotype data linked to electronic health records, family history, and aortic tissue from individuals seen at Michigan Medicine. The Michigan Genomics Initiative (MGI) is a hospital-based cohort with genotype data linked to electronic health records from individuals recruited during pre-surgical encounters at Michigan Medicine. Both studies were approved by the Institutional Review Board of the University of Michigan Medical School (IRBMED) (HUM00052866 and HUM00071298) and informed consent was obtained from study participants.

Genotype, QC, and imputation

CHIP and MGI samples were genotyped with two array versions of customized Illumina Infinium CoreExome-24 bead arrays: UM_HUNT_Biobank_11788091_A1 and UM_HUNT_Biobank_v1-1_20006200_A. A detailed description of these two arrays can be found in Fritsche et al.[10] Genotype calling was performed with Illumina GenomeStudio. Extensive quality control (QC) was performed prior to imputation. For CHIP samples, we first excluded samples with (1) rotated/swapped plates or DNA extraction batches, (2) duplicate/redundant samples with lower call rate, (3) identical ID and discordant genotypes or different ID but identical genotypes (both samples excluded), (4) gender discordance (unusual XY composition/no gender information available; no gender check possible/reported gender different from inferred sex), (5) large copy number variant, (6) estimated contamination $>$ 2.5% (BAF Regress[11]), and (7) sample call rate $<$ 99%. In all samples, we excluded variants with (1) call rate $<$ 90%, (2) GenTrain score $<$ 0.15, and (3) cluster separation $<$ 0.3. After this, individual batches in each array version were merged. We also obtained MGI samples with similar processing as described in Fritsche et al.[10] Next, from three sets (two CHIP array versions and MGI), we excluded samples with (1) outlier heterozygosity and (2) non-European ancestry as identified by laser[12] and variants with (1) call rate $<$ 99% or (2) deviation from Hardy-Weinberg equilibrium (p value $< 10^{-4}$). Further analysis was restricted to variants present in both the MGI and two CHIP array versions among unrelated ($>3^{rd}$ degree) individuals identified via KING.[13] Variants with allele frequency differences between two array versions in CHIP (Chi-square; $p < 0.001$) were removed. Monomorphic variants were also excluded at this stage, generating 457,758 polymorphic variants from 42,119 samples after QC. As a preparation for imputation with the Haplotype Reference Consortium (HRC) panel,[14] we further excluded 71,942 variants from this set by using McCarthy group tools. The 385,816 variants that passed QC were used as input in the Michigan Imputation server. Imputation was performed with the HRC reference panel via Minimac4[15] with Rsq filter 0.3.

Case-control selection and association analysis

TAA-affected individuals were identified from both CHIP and MGI while control individuals were identified from MGI. Affected individuals in CHIP (n = 956) were defined as having an aneurysm in the thoracic aorta following diagnosis by cardiologists. Individuals with a known diagnosis of BAV were excluded because this is a strong risk factor of TAA, presumably because of altered haemodynamic blood flow and aortopathy instead of shared genetic architecture or molecular mechanisms.[16,17] Affected individuals in MGI (n = 395) were identified via International Classification of Diseases (ICD) codes (ICD9, 441.1/441.2; ICD10, I71.1/I71.2) excluding samples with a diagnosis of BAV (ICD9, 746.4; ICD10, Q23.1). After removing samples with any related diseases from the potential control individuals (phecodes 440–449.99), we used a case-control matching strategy to identify 18,295 control individuals from MGI (Table S1). We used R package MatchIt and applied nearest neighbor matching for birth year, PC1–4 (using Mahalanobis-metric matching), and exact matching for sex and array version. Association analysis was performed via SAIGE[18] with sex, birth year, array version, and PC1–4 as covariates. We reported results for all variants with minimum minor allele frequency (MAF) of 0.01 and minor allele count of 5.

Replication data and meta-analysis

The replication study from the University of Texas Health Science Center at Houston was approved by the institutional review board (IRB) (HSC-MS-01-251) and all subjects signed consent forms at recruitment to the study. The phenotyping and case-control association analysis is described in LeMaire et al.[8] Briefly, this data comprises 765 individuals of European ancestry with sporadic ascending aortic aneurysms or classic aortic dissection of the ascending or descending thoracic aorta (Stanford types A and B, respectively) and 875 control individuals. A logistic regression model was used for testing of variant association with the phenotype.

The VA Million Veteran Program (MVP) is comprised of veterans aged 18 to $>$100 years recruited from VA healthcare centers across the United States with genetic data linked to electronic health records. The study was approved by the VA central IRB and all participants provided informed consent. In MVP, 6,554 unrelated TAA-affected individuals of European ancestry were identified on the basis of the occurrence of a TAA ICD code (ICD9, 441.1/ 441.2; ICD10, I71.1/I71.2) on two distinct dates (individuals with BAV

were excluded; ICD9, 746.4; ICD10, Q23.1) and compared to 329,971 unrelated control individuals who were free of any codes listed in Table S2. Genotyping, imputation, and genomic quality control was performed as described elsewhere.[19] DNA variants were tested for their association with TAA via logistic regression in PLINK2 and controlled for age at time of analysis, age, gender, HARE ancestry assignment,[20] and the first five genetic principal components of ancestry (PCAs). Sensitivity analyses were then performed with participants who had undergone any form of thoracic aortic repair and subgroups of ascending and arch repair as cases based on Current Procedural Terminology (CPT) codes provided in Table S2. Covariates and controls were included in the same manner as the primary analysis.

The Trøndelag Health Study (the HUNT Study)[21] is a longitudinal population-based health survey conducted in Norway. Participation in the HUNT Study is based on informed consent, and the study has been approved by the Norwegian Data Protection Authority and the Regional Ethics Committee for Medical Research in Norway. Genotyping, quality control and imputation is described elsewhere.[22] We used ICD9 441.1/441.2 and ICD10 I71.1/I71.2 to identify 380 affected individuals and 69,255 control individuals from HUNT. Association analysis was performed via SAIGE[18] v.43.3 with sex, birth year, batch, and four PCs as covariates.

The UK Biobank[23] is a population-based cohort collected from multiple sites in the United Kingdom. We used ICD10 I71.1/I71.2 (excluding Q23.1) to identify 220 affected individuals among those of white British ancestry. After excluding samples with ICD10 I71.0–I71.9, 3,253 control individuals were selected by case-control matching as described in the discovery cohort. Association analysis was performed via SAIGE[18] with sex, birth year, array version, and four PCs as covariates.

Meta-analysis of three variants in the discovery and replication cohorts was performed by METAL[24] with the standard error approach.

Additional datasets

We downloaded the T2D GWAS in Europeans as "Mahajan.NatGenet2018b.T2D.European.gz" from the DIAGRAM consortium. The eQTL data in aorta as "Artery_Aorta.v8.signif_variant_gene_pairs.txt.gz" and "GTEx_v8_finemapping_CAVIAR.tar" were downloaded from the GTEx portal. DNase I hypersensitive site and H3K27ac of thoracic/ascending aorta (Table S3) were obtained from ENCODE. Promoter capture Hi-C data, as described in Jung et al.,[25] were obtained as "AO.po.txt.zip."

Conditional analysis

Approximate conditional analyses were performed with GCTA.[26] We used the –cojo-cond option to run conditional analyses with specific variants. We used the full summary statistics but limited the analysis to ± 500 kb of the conditional variant by using the –extract-region-snp parameter. For conditional analysis, imputed variants from CHIP+MGI (European ancestry) were used as the linkage disequilibrium (LD) reference. We reported the p value of rs7903146 in T2D GWAS conditional on rs4073288 and the p value of rs4073288 in TAA GWAS conditional on rs7903146 and other T2D variants (Table S4).

Colocalization

Colocalization analyses were performed with the R package coloc.[27] Coloc performs an approximate Bayes factor analysis with association statistics. We used the function coloc.abf()to calculate the posterior probabilities for the following: (H0) no association with either trait, (H1/H2) association with one of the two tested traits, (H3) association for both traits but different causal variants, and (H4) association for both traits with the same causal variant. A high posterior probability for H4 (PP4) indicates colocalization of the two trait associations. Variants in the ± 500 kb region surrounding rs4073288 were used for colocalization. The default prior probability for colocalization was used for both T2D and eQTL analyses.

Transcriptome-wide association study

To evaluate the evidence of colocalization between the TAA GWAS and eQTL association, we used the paradigm of transcriptome-wide association study (TWAS). TWAS methods perform gene-based association tests. We used these methods to test the association between gene expression predicted by cis-eQTLs and phenotype. We used the MetaXcan package[28] to run TWAS with TAA summary statistics. Briefly, we used GWAS tools from the MetaXcan package for summary statistics harmonization and imputation. The imputation step imputes missing GWAS variants via present GWAS variants and the GTEx genotypes. Next, we ran SPrediXcan with the imputed variants and the MASHR expression model (eQTL) of aorta from GTEx v.8.[29] We reported the Z scores and p values from this analysis. We did not observe any inflation of test statistics ($\lambda = 0.99$). No other genes except *TCF7L2* had significant association after multiple testing correction for 13,951 genes present in the aortic expression model (p value significance threshold; $0.05/13{,}951 = 3.58 \times 10^{-6}$).

Fine-mapping

We employed FINEMAP,[30] a Bayesian fine-mapping method that implements a stochastic shotgun search algorithm incorporating the LD structure and associations (Z scores) in a locus, to identify potential causal variants. Variants with MAF > 5% in the ± 500 kb surrounding rs4073288 were used for this analysis. The LD structure in this locus was determined via PLINK[31] from imputed variants in CHIP/MGI. The fine-mapping was carried out with the assumption of a single causal variant. We constructed the 95% credible set by including the variants with highest posterior probabilities and until the sum of posterior probabilities was ≥0.95. We used RegulomeDB[32] to annotate variants. RegulomeDB uses public databases to aggregate information about eQTL, transcription factor binding/motif, DNase peak/footprint, etc. for each tested variant. The method assigns a rank to each variant that represents the likelihood of a variant's being a regulatory variant. We prioritized two variants by using this approach (Table S5). Because RegulomeDB operates in a tissue-agnostic manner, we checked the overlap of fine-mapped variants with the DNase I hypersensitive site and H3K27ac of thoracic/ascending aorta from ENCODE.[33] We configured custom tracks in UCSC genome browser to visualize the overlap of variant and chromatin marks. We obtained the promoter capture Hi-C in aorta from Jung et al.[25] The p values of chromatin interaction between promoter (chr10: 114,703,220–114,715,198) and variant (respective genomic bin) were reported.

LD score regression (LDSC)

We used "munge_sumstats.py" in LDSC[34] to format summary statistics. For further analyses, only variants with MAF > 0.01 and imputation Rsq > 0.9 and that were from Hapmap3 were incorporated. Heritability calculation was performed via the –h2 parameter (with –samp-prev and –pop-prev) in LDSC. Genetic correlations

between TAA and other traits were calculated in LD Hub.[35] Sources of summary statistics of these traits are listed in Table S6.

Adenoviruses

The Myc-tagged human full-length *TCF7L2* pcDNA3 plasmid was previously reported[36] (Addgene plasmid # 32738; RRID: Addgene_32738). The coding region of Myc-TCF7L2 from that plasmid was cloned into PCR8/GW/TOPO TA (entry) vector (K250020, Thermo Fisher Scientific) and recombined from the entry vector to the pAd/CMV/V5-DEST Vector (V49320, Thermo Fisher Scientific). The adenovirus carrying LacZ was described before.[37] The adenoviruses were packaged in HEK293A cells and purified by $CsCl_2$ density gradient ultracentrifugation. Adenovirus titration was determined by the Adeno-XTM quantitative PCR titration kit (Clontech, CA, USA).

Cell line growth and *TCF7L2* gain and loss of function *in vitro*

Primary human aortic smooth muscle cells (HASMCs) (Lonza, CC2571, lot # 000335663, Walkersville, MD, USA) were grown in smooth muscle cell growth medium 2 containing 5% fetal bovine serum (PromoCell, Germany) and 1% penicillin/streptomycin solution (GIBCO, #15140122) at 37°C with 5% CO_2 in a humidified incubator and subjected to quiescence in Opti-MEM for 48 h when so required. HASMCs were used from passage 5 to 8. For overexpression of *TCF7L2*, adenoviruses containing myc-tagged *TCF7L2* or LacZ (control) under the control of the cytomegalovirus (CMV) promoter were used for infection at 30 MOI. For knockdown, cells were transfected with siRNA against *TCF7L2* (Horizon D-003816-01 sequence: GAUGGAAGCUUACUAGAUU) or siRNA control (Horizon D-001206-14) at a concentration of 30 nM with Lipofectamine RNAiMAX for 72 h in serum-free medium (Opti-MEM) before use for apoptosis studies.

Apoptosis studies

HASMCs with gain or loss of TCF7L2 as above were treated with 100 ng/mL Fas ligand (FasL) (Enzo Life Science: ALX-522-020) for the indicated times in Opti-MEM, as we previously reported[37] (48 h after adenoviral infection or 72 h after siRNA treatment). For annexin V studies, cells were treated for 4 h with FasL in Opti-MEM medium (31985062, GIBCO). Cells were dissociated with 0.25% trypsin (25200056, GIBCO) and stained with the FITC Annexin V Apoptosis Detection Kit I (556548, BD Biosciences), as we previously reported.[37] In brief, the cells were washed with cold PBS twice, suspended in 1× binding buffer and stained with FITC annexin V and propidium iodide (PI). The flow cytometry analysis was performed by the flow cytometry core at the University of Michigan with a MoFlo Astrios Cell Sorter (Beckman Coulter, Brea, CA). Apoptotic cells are defined as FITC annexin V positive and PI negative. For immunoblot, cells were treated for 6 h with FasL and subjected to immunoblot with standard protocols as described below.

Quantitative real-time PCR and immunoblot

HASMCs were grown and treated as indicated in each case. For quantitative real-time PCR, we isolated total RNA from HASMCs with the RNeasy Mini Kit (QIAGEN, #74106) followed by the SuperScript III First-Strand Synthesis System (Invitrogen, #18080051) by using random hexamers to generate cDNA, as suggested by the respective manufacturers. Gene expression was quantified in triplicates by quantitative real-time PCR with IQ SYBR Green Supermix (Bio-Rad, #1708882). Relative levels were determined via the ΔΔCt method with expression of the *ACTB* (Actin Beta) gene as the internal control. The qPCR primer sequences are listed in Table S7. For immunoblot, cell extracts were prepared with RIPA lysis buffer supplemented with complete EDTA-free protease inhibitor cocktail (Roche, #11836170001, Penzberg, Germany) and PhosSTOP phosphatase inhibitor (Roche, #4906845001). The protein concentration was determinedwith the Bradford assay (Bio-Rad, #5000002) and a GloMax Explorer Multimode Microplate Reader. A total of 40 μg of total protein/lane was resolved in SDS-PAGE gels (Bio-Rad 4561094) and transferred to nitrocellulose membranes (Bio-Rad, #1620115, Hercules, CA) with standard techniques. Antibodies were used as follows: the BCL2 antibody (ab182858, 1.2 μg/mL) from Abcam (UK); β-actin (#3700, 0.65 μg/mL), PARP (#9542, 0.1 μg/mL), Caspase 3 (#9662, 0.05 μg/mL), cleaved Caspase 3 (#9664, 0.04 μg/mL), BAX (#5023, 0.14 μg/mL), and myc (#2276, 0.3 μg/mL) from Cell Signaling Technology (CST, Danvers, MA); and the secondary antibodies, IRDye 800CW Donkey anti-Rabbit IgG and IRDye 680RD Donkey anti-Mouse IgG at 0.2 μg/mL, from LI-COR Bioscience (Lincoln, NE). We collected data by using the Odyssey CLx Imaging System (LI-COR Bioscience) and quantified data with the LI-COR Image Studio Software to determine the protein abundance relative to β-actin.

Results

We performed genetic discovery association analysis of 1,351 affected individuals and 18,295 control individuals (European ancestry) from the Cardiovascular Health Improvement Project (CHIP) and Michigan Genomics Initiative (MGI) at the University of Michigan, Michigan Medicine. Imputation with the HRC panel in the Michigan Imputation Server enabled testing of 22.9 million variants. We did not observe any evidence of inflation ($\lambda_{GC} = 1.04$) of the association test statistics (Figure S1A). Using LD score regression with sample- and population-level prevalence (6% and 0.34%,[38] respectively), we estimated SNP heritability of TAA as 0.11 (SE = 0.04) in liability scale. Next, genetic correlation between TAA and known risk factors was examined with GWAS summary statistics (Table S6). We observed a positive genetic correlation between TAA and height ($r_g = 0.32$, SE = 0.11, p = 0.003). This correlation remained significant after excluding variants within 500 kb from rs591519 (*FBN1*, a gene associated with Marfan syndrome and related disorders) from TAA summary statistics. We did not observe a significant genetic correlation between TAA and smoking or lipid traits, two factors strongly correlated with abdominal aortic aneurysm (AAA).[39] On the contrary, diastolic blood pressure is positively correlated with TAA ($r_g = 0.27$, SE = 0.09, p = 0.003) but systolic blood pressure is not ($r_g = -0.006$, SE = 0.08, p = 0.93).

Association with TAA at the *TCF7L2* locus

57 variants from two loci reached genome-wide significance ($p < 5 \times 10^{-8}$) in our analysis (Figure S1B). First, we replicated a significant association at the previously known *FBN1* locus (index variant rs591519, A/T, effect allele: T, β = 0.42, SE = 0.06, OR 95% CI = 1.35–1.71,

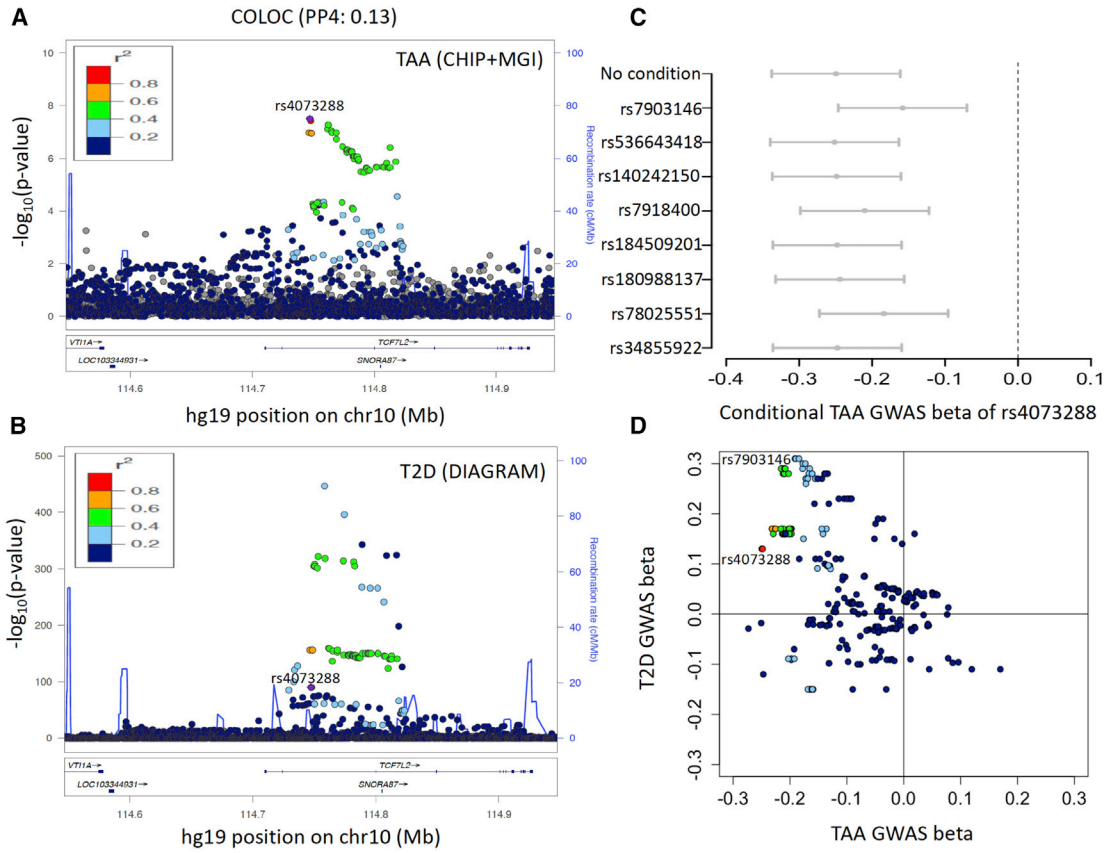

Figure 1. *TCF7L2* locus in TAA and T2D

(A) LocusZoom plot of *TCF7L2* locus in TAA GWAS from CHIP+MGI.

(B) LocusZoom plot of *TCF7L2* locus in T2D GWAS from DIAGRAM. LD colors are with respect to the TAA index variant rs4073288.

(C) Conditional effect sizes (beta, in SD units) of TAA index variant rs4073288 in TAA GWAS. Eight independent T2D variants were used for conditioning. Error bars represent 95% confidence intervals.

(D) Comparison of effect sizes (beta) in TAA and T2D GWAS. Variants in this locus have opposite direction in effect sizes in TAA versus T2D GWAS.

$p = 1.1 \times 10^{-9}$). Second, we identified a previously unpublished TAA association in the intronic region of *TCF7L2* in chromosome 10 (Figure 1A). The index variant rs4073288 (Table 1) is a common variant with an MAF of 0.32 in cases and 0.37 in controls. We observed 49 common variants (MAF range: 0.37–0.47) with $p < 5 \times 10^{-6}$ in this locus (three genotyped; 46 imputed, Rsq: 0.88 to 0.94). A conditional analysis on rs4073288 did not identify any secondary independent variants in this locus. At both the *TCF7L2* and *FBN1* loci, we observed a reduced effect in MGI compared to CHIP cases (Table S8). Among 956 CHIP cases, approximately 80% and 8% were classified as ascending and descending TAA, respectively. Interestingly, at the *TCF7L2* locus, we observed stronger effect in descending TAA, while the *FBN1* effects were stronger in ascending TAA (Table S8). We observed lower effects in the same direction for association with AAA[39] at *TCF7L2* (rs4073288, effect allele: A, $\beta = -0.05$, SE = 0.02, OR 95% CI = 0.91–0.99, $p = 3.1 \times 10^{-3}$) as well as *FBN1* (rs591519, effect allele: T, $\beta = 0.06$, SE = 0.03, OR 95% CI = 1–1.13, p = 0.03). These variants were not significant ($p > 0.05$) for association with intracranial aneurysm.[40]

Next, we sought replication of the *TCF7L2* locus in a meta-analysis of four independent datasets of European ancestry from (1) University of Texas Health Science Center at Houston (UT, 765 affected individuals), (2) The Trøndelag Health Study (the HUNT Study, 380 affected individuals), (3) UK Biobank (220 affected individuals), and (4) the Million Veteran Program (MVP, 6,554 affected individuals). We observed consistent direction of effect sizes in all replication cohorts (Figure S2). At both the *TCF7L2* and *FBN1* loci, substantial differences in effect estimates among cohorts were observed (Figure S2). *TCF7L2* effect estimates were similar between the Michigan discovery and UT datasets, two cohorts that were primarily ascertained from aortic clinics, whereas the other datasets used ICD-based phenotypes from large biobanks. In MVP, we further identified a smaller subset of TAA-affected individuals in whom surgical repair was performed (730 affected individuals). We observed stronger effect estimates in these affected individuals compared to ICD-based phenotypes (three *TCF7L2* variants, OR = 0.86–0.89 for surgical repair TAA versus OR = 0.94 for all ICD-derived TAA-affected individuals; Table S9). This observation highlights the

Table 1. Discovery and replication of *TCF7L2* variants in TAA

			Discovery				Replication				Discovery + replication			
Variant	**EA**	**OA**	**Beta**	**SE**	**OR 95% CI**	**p**	**Beta**	**SE**	**OR 95% CI**	**p**	**Beta**	**SE**	**OR 95% CI**	**p**
rs4073288 (index)	A	G	−0.25	0.04	0.72–0.84	3.1×10^{-8}	−0.07	0.02	0.90–0.97	4.2×10^{-5}	−0.10	0.02	0.87–0.94	5.2×10^{-9}
rs7904519 (genotyped)	G	A	−0.21	0.04	0.75–0.88	3.6×10^{-7}	−0.07	0.02	0.90–0.97	1.7×10^{-5}	−0.09	0.01	0.90–0.93	3.3×10^{-9}
rs4074718 (fine-mapped)	A	G	−0.23	0.04	0.73–0.86	1.1×10^{-7}	−0.07	0.02	0.90–0.97	4.0×10^{-5}	−0.09	0.02	0.88–0.95	5.8×10^{-9}

EA, effect allele; OA, other allele.

limitation of replication with cohorts with different phenotype definitions and/or case-ascertainment strategies. Nonetheless, after combining all replication datasets, we observed an association p value $< 5 \times 10^{-5}$ for all three tested variants at *TCF7L2* (Table 1).

Comparison of the *TCF7L2* association with TAA and type 2 diabetes

TCF7L2 is known to be associated with T2D.[41] A common variant in the 3rd intron of *TCF7L2* is associated with T2D and most likely causes a defect in insulin secretion in the pancreas.[42] The TAA index variant rs4073288 is in relatively low LD with the T2D index variant rs7903146 ($R^2 = 0.28$ in Europeans, ~11 kb apart, 3rd intron). We further examined GWAS summary statistics of T2D from Mahajan et al.[43] (rs7903146, $P_{T2D} = 1.5 \times 10^{-447}$; rs4073288, $P_{T2D} = 3.8 \times 10^{-91}$) (Figure 1B). Although the same region within *TCF7L2* (3rd intron) is associated with both TAA and T2D risk, the posterior probabilities from co-localization analysis indicated independent signals for TAA and T2D (COLOC, PP3 = 0.85, PP4 = 0.13). Also, a reciprocal conditional analysis did not diminish either signal completely (TAA, $P_{cond:rs7903146}$ rs4073288 $= 4.5 \times 10^{-4}$; T2D, $P_{cond:rs4073288}$ rs7903146 $= 3.4 \times 10^{-262}$). Mahajan et al. reported seven other secondary independent variants associated with T2D in this locus, which may be functional in different tissues.[43] All of these secondary T2D variants have very low correlation with the TAA index variant rs4073288 (maximum $R^2 = 0.24$; Table S4). The association between rs4073288 and TAA remained significant when we conditioned on each of these eight T2D variants (Figure 1C). These observations suggest the presence of different causal variants for TAA and T2D. Finally, we noted an opposite direction of effect (Figure 1D) for TAA and T2D at variants in this region (rs4073288, effect allele: A, $\beta_{TAA} = -0.24$ [0.04], $\beta_{T2D} = 0.13$ [0.006]; rs7903146, effect allele: T, $\beta_{TAA} = -0.18$ [0.04], $\beta_{T2D} = 0.31$ [0.006]). The opposite direction of effect for T2D and TAA was consistent in all variants with $P_{TAA} < 5 \times 10^{-6}$ in this locus. We did not observe a significant genetic correlation between TAA and T2D ($r_g = 0.006$, SE = 0.15, p = 0.96) via GWAS summary statistics.

Higher expression of *TCF7L2* in aorta is associated with TAA risk

To investigate a potential effect of TAA GWAS variants on expression of *TCF7L2*, we looked for tissue-specific cis-eQTLs from GTEx v.8.[29] The TAA index variant rs4073288 is an eQTL of *TCF7L2* in aorta (effect allele: A, normalized effect size = −0.27, $p = 2.6 \times 10^{-11}$, N = 387). The TAA risk allele (G in rs4073288) is associated with higher expression of *TCF7L2* in aorta (Figure S3A). This eQTL association was not observed in any other tissue (Figure S3B). Further analysis revealed colocalization (Figure 2B) between the GWAS and eQTL signal (COLOC, PP3 = 0.03, PP4 = 0.96). Next, we performed a TWAS analysis by using SPrediXcan[28] with the MASHR aortic expression model from GTEx v.8. This resulted in a significant association between predicted expression levels of *TCF7L2* and TAA (Z score = 5.35; $p = 8.38 \times 10^{-8}$; Bonferroni corrected threshold: $0.05/13{,}951 = 3.58 \times 10^{-6}$; Figure S3C). A positive Z score in TWAS indicated that higher expression of *TCF7L2* is associated with TAA disease. This observation suggests a probable disease mechanism of TAA-associated variants via an increase of *TCF7L2* expression in aorta.

Investigation of the causal variant in the *TCF7L2* locus

We hypothesize that the TAA causal variant affects the expression of *TCF7L2* via alteration of some regulatory element in this region. In an attempt to identify the causal variant, we applied a Bayesian fine-mapping approach, FINEMAP.[30] The 95% credible set for the GWAS consisted of 32 variants from this locus. We also obtained the fine-mapped variants in eQTL by CAVIAR[44] from GTEx. Out of 32 variants in the GWAS credible set, 23 were also present in the 95% causal set of eQTL (Figure S4A). Next, we used RegulomeDB[32] to annotate variants with known or predicted regulatory elements. We could further prioritize (Table S5) two variants in the common credible set (Figure 2B). Both these variants (rs4074718 and rs4077527) have larger effect sizes for the *TCF7L2* eQTL than the index variant rs4073288. While both variants are from regions annotated as enhancers in multiple tissues, rs4077527 intersects with accessible chromatin (DNase I hypersensitive site) in adult thoracic/ascending aorta in ENCODE[33] data (Figure 2C, Table S3). We also observed strong evidence of enhancer activity (H3K27ac) in these samples overlapping rs4077527. Because both these variants are quite far from the *TCF7L2* promoter (rs4074718, ~40 kb; rs4077527, ~10 0kb), we examined promoter capture Hi-C data from aorta.[25] A significant long-distance chromatin interaction ($p < 0.01$, as per methods in Jung et al.[25])

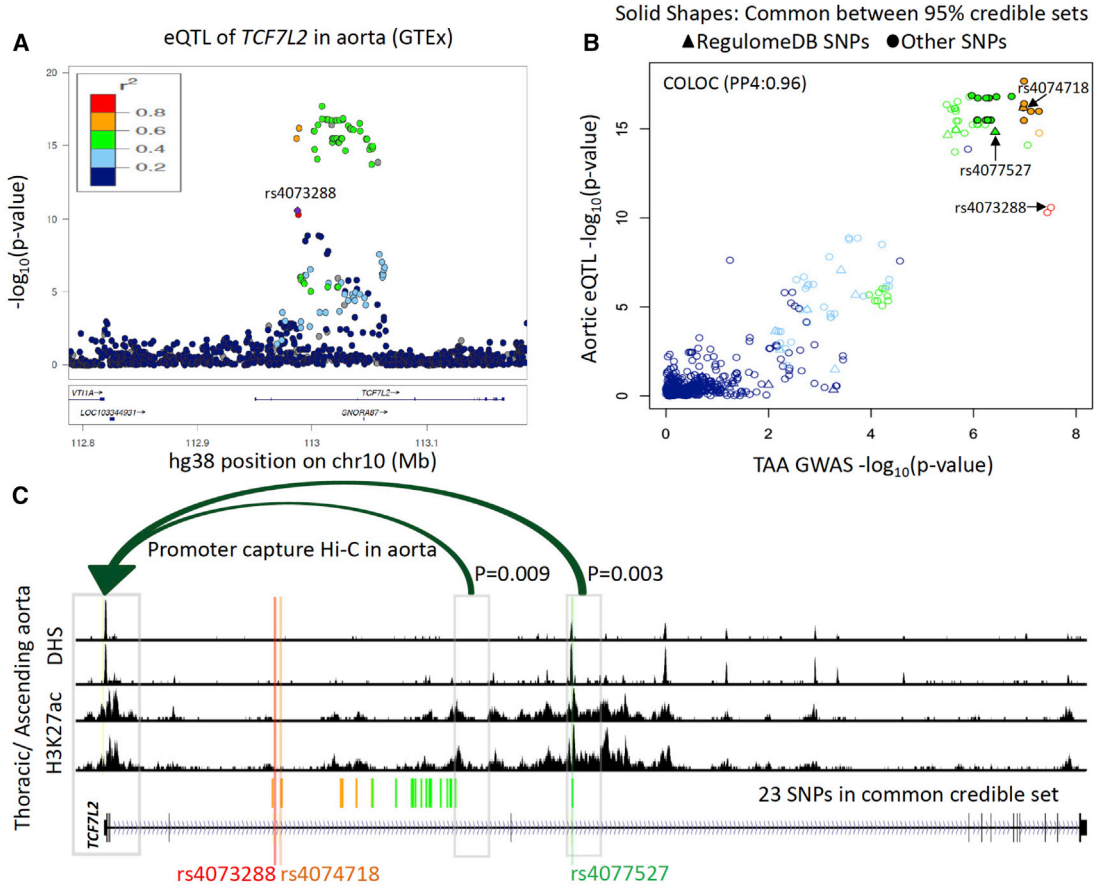

Figure 2. Functional characterization of *TCF7L2* locus

(A) LocusZoom plot of aortic eQTL of *TCF7L2*. LD colors are with respect to the TAA index variant rs4073288.

(B) Comparison of p values in TAA GWAS and aortic eQTL from GTEx. These two associations colocalize with posterior probability 0.96 by COLOC. The solid shapes represent 23 variants that were in both GWAS and eQTL 95% credible sets. Two variants were prioritized by RegulomeDB (rs4074718 and rs4077527).

(C) Regulatory landscape of *TCF7L2* gene body in thoracic aorta/ascending aorta from ENCODE. The fine-mapped variant rs4077527 intersects with DNase I hypersensitive site (DHS) and H3K27ac in this tissue. Using promoter capture Hi-C in aorta, we highlighted only genomic bins that significantly interact ($p < 0.01$) with *TCF7L2* promoter. Promoter capture Hi-C p values for 23 variants are given in Figure S4B.

between rs4077527 and the *TCF7L2* promoter region (hg19; chr10: 114,703,220–114,715,198) was observed (Figure 2C, Figure S4B). Together, these observations predict rs4077527 as a strong candidate for the causal TAA variant in this locus, most likely interacting with the promoter to impact *TCF7L2* expression in the aorta.

TCF7L2 enhances human vascular smooth muscle cell apoptosis

TAA is characterized by vascular smooth muscle cell (VSMC) apoptosis in association with loss of their contractile phenotype, inflammatory status, and increased extracellular matrix degradation as drivers of adverse outcomes.[45] Loss of VSMC in TAA is recognized to be the result of increased apoptosis through the endogenous pathway regulated via *BCL2*.[45,46] As a distal effector of the Wnt/β-catenin/TCF-LEF pathway, *TCF7L2* is known to regulate homeostasis of VSMC, the media layer of blood vessels, including phenotypic modulation and proliferation.[47–49] *TCF7L2* may exert pro-[50,51] or anti-apoptotic[52,53] effects in different contexts. Yet, contribution of *TCF7L2* to VSMC apoptosis in aneurysm remains unaddressed. We experimentally assessed whether gain and loss of function of *TCF7L2* contributes to VSMC apoptosis via differential regulation of *BCL2* expression in human aortic smooth muscle cells (HASMCs) *in vitro*. Adenoviral-mediated overexpression of *TCF7L2* resulted in reduced *BCL2* expression of both mRNA (54% reduction, $p = 0.0004$) and protein (24% reduction, $p = 0.0011$) (Figures 3A and 3B, Figure S5A) compared with the adenoviral-mediated expression of LacZ used as control. Conversely, siRNA-mediated downregulation of *TCF7L2,* which resulted in a significant reduction in endogenous *TCF7L2* mRNA (80% reduction, $p = 0.0002$ versus siRNA control) and protein (77% reduction, $p = 0.0145$ versus siRNA control), demonstrated a concomitant increase in *BCL2* protein (1.6-fold increase, $p = 0.0154$ versus shRNA control) and mRNA abundance (2.7-fold increase, $p = 0.0001$) (Figures 3C and 3D, Figure S5B). Changes in *TCF7L2* showed no significant effects on BAX protein or mRNA expression (Figures 3A–3D,

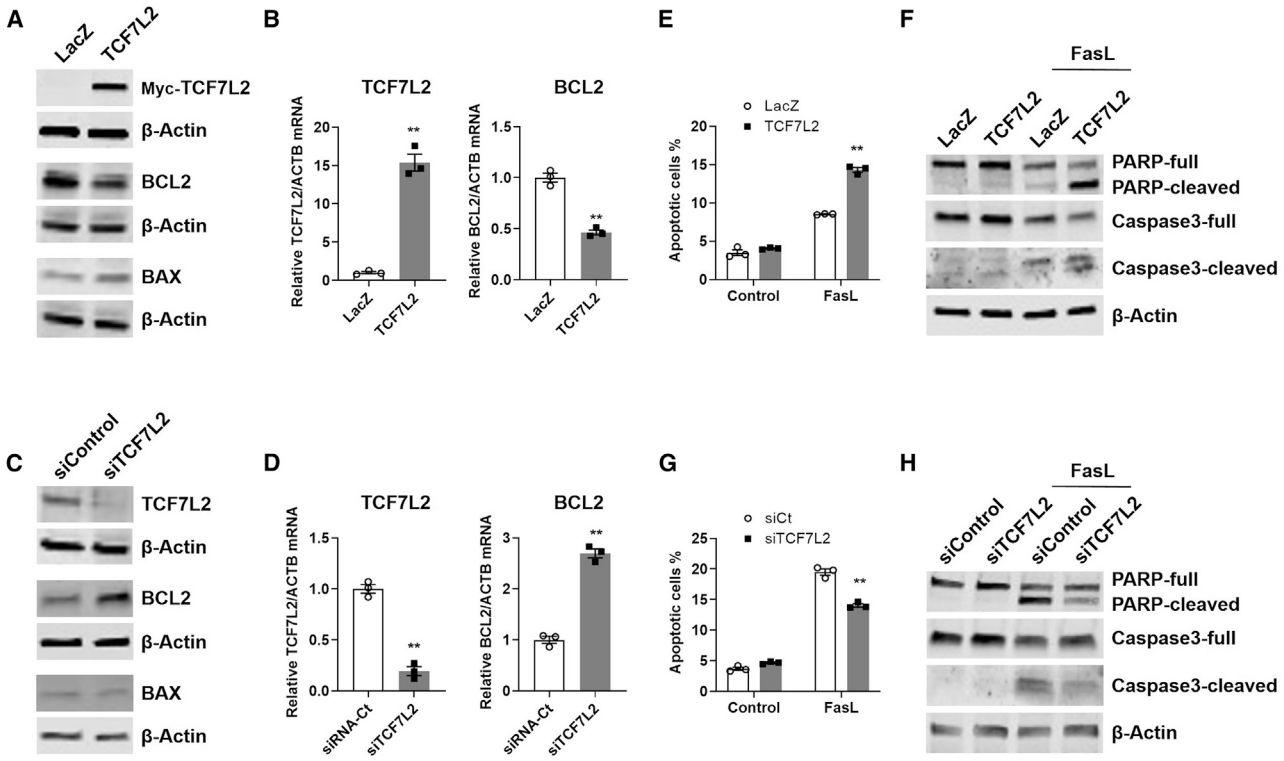

Figure 3. ***TCF7L2* expression is directly associated with vascular smooth muscle cell apoptosis *in vitro***
HASMCs were infected with adenovirus (30 MOI)-encoding LacZ (control) or myc-tagged *TCF7L2*, and after 48 h, (A) the abundance of the indicated proteins in the cell extracts was determined by immunoblot (representative of three independent experiments) and (B) the mRNA expression of the indicated genes, relative to ACTB, by quantitative real-time PCR. A LacZ control was set at 1 as reference ($n = 3$; representative of three independent experiments). Data are mean ± SEM. $^{**}p \leq 0.0004$. HASMCs were transfected with siRNA control or siRNA against *TCF7L2* via Lipofectamine RNAiMax, and after 72 h, (C) the abundance of the indicated proteins and (D) the mRNA expression of the indicated genes were determined as described above with an siRNA control set at 1 as reference. $^{**}p \leq 0.0002$. HASMCs were infected with adenovirus as in (A). After 48 h in serum-free medium, they were treated with Fas ligand (FasL, 100 ng/mL) in serum-free medium and apoptosis was assessed by (E) annexin V via FACS analysis after treatment for 4 h ($n = 3$; representative of three independent experiments) or (F) the abundance of the indicated proteins in the cell extracts after 6 h as determined by immunoblot (representative of three independent experiments). HASMCs were transfected with the indicated siRNA as in (C). After 72 h in serum-free medium, they were treated with FasL (100 ng/mL) for (G) annexin V assay after 4 h as in (E) or (H) immunoblot after 6 h as in (F) and subjected to immunoblot as in (E). Densitometry for (A), (B), (E), (F), and mRNA expression of *BAX* are provided in Figure S5.

Figures S5A–S5D). Consequently, we determined a significant BAX/BCL2 protein ratio between *TCF7L2* overexpression and knockdown (1.3222 ± 0.1024 versus 0.6426 ± 0.1176, $p = 0.0168$, respectively) in basal growth conditions (Figures 3A and 3B, Figure S5A), suggesting a potential pro-apoptotic effect of *TCF7L2* upregulation in HASMCs.

We further examined the expectation that increased *TCF7L2* expression enhances apoptosis of aortic smooth muscle cells through treatment with FasL, a potent inducer of VSMC apoptosis produced by inflammatory cells in the aneurysmal tissues.[45,54] In these experimental conditions, FasL treatment resulted in significant increase in annexin V positive cells (1.7-fold, $p \leq 0.0001$), indicative of enhanced early apoptosis when *TCF7L2* was overexpressed (Figure 3E, Figure S5E), while siRNA-mediated *TCF7L2* knockdown significantly reduced the apoptotic response by 28% ($p \leq 0.0001$) (Figure 3G, Figure S5F), as determined by fluorescence-activated cell sorting (FACS). These data were in agreement with progression into apoptosis upon *TCF7L2* overexpression, as indicated by significantly increased cleavage of PARP and caspase-3 compared to the corresponding full-length proteins (Figure 3F, Figure S5G). Conversely, siRNA-mediated knockdown of *TCF7L2* significantly reduced cleavage of both apoptosis markers (Figure 3H, Figure S5H). Overall, these data indicate that increased expression of *TCF7L2* may result in enhanced apoptosis of vascular smooth muscle cells—a likely mechanism of action of TAA-associated variants in *TCF7L2*.

Discussion

In this study, we identified a locus in the intronic region of *TCF7L2* that is associated with TAA, to our knowledge, the first locus identified for TAA via genome-wide approaches. Using eQTL from aorta, we provide evidence that TAA-associated variants are associated with altered expression of *TCF7L2* and we highlight one variant in the locus that overlaps with an enhancer active in aorta. Common variants (rs7903146, index variant) in this locus are

the strongest known genetic risk factor for T2D.[42] Vinuela et al.[55] demonstrated that the T2D risk allele of rs7903146 decreases pancreatic islet expression of the last (3′) exon of *TCF7L2*. Although there is evidence of different causal variants for TAA and T2D, we observed an opposite direction in effect sizes. Interestingly, epidemiological studies have historically suggested an inverse relationship between aortic aneurysm and T2D.[56–58] Our genetic results suggest that, at least for the *TCF7L2* locus, shared but independent etiology (gene-level horizontal pleiotropy) may be partially responsible for this association. These results most likely indicate that largely independent sets of causal variants lead to increased *TCF7L2* expression in the human aorta and decreased *TCF7L2* expression in pancreatic islets.

The T-cell factor/lymphoid enhancer factor (TCF/LEF) transcription factors (including *TCF7L2*) are signal integrators and effectors of the Wnt/β-catenin pathway with contextual tissue and cell-type-specific functions[59] and can exhibit differential effects because of epigenetic modifications of the target genes. Wnt/β-catenin is an evolutionarily conserved pathway that regulates various aspects of development, including cell proliferation, migration, polarity, and apoptosis.[60] Dysregulation of the Wnt/β-catenin signaling is involved in a wide range of disorders, including Alzheimer disease, cancer, and metabolic diseases.[61] Current research supports a role of *TCF7L2* in vascular development.[62–64] In cardiovascular diseases, the Wnt/β-catenin pathway was found to be dysregulated in restenosis,[65] and more recently, *TCF7L2* was demonstrated to regulate VSMC plasticity in both *GATA6*-dependent and -independent fashions.[47] Regarding aneurysm, Krishna et al. reported activation of the Wnt/β-catenin pathway in AAA via epigenetic silencing of the Wnt inhibitor sclerostin.[66] Recently, dysregulated Notch/BMP/WNT pathways were found in aortic endothelial cells isolated from individuals with TAA compared to healthy donors,[67] including increased *TCF7L2* mRNA expression and activation of the Wnt/β-catenin pathway in the endothelium. Our analyses indicate that variants associated with higher expression of *TCF7L2* are also associated with TAA. TAA is a disease characterized by VSMC death as a driver of adverse outcomes.[45] Therefore, we specifically addressed the potential effects of *TCF7L2* on VSMC apoptosis *in vitro*. We show that *TCF7L2* expression is directly associated with VSMC apoptosis and that this effect could be mediated, at least in part, through *TCF7L2* repression of *BCL2* expression, a known target of the pathway. Our data from VSMC, together with the report from endothelial cells,[67] clearly indicate that upregulation of *TCF7L2* may play a fundamental role in TAA pathology.

Mendelian, monogenic inheritance of TAA is primarily driven by pathogenic variants in genes from the TGF-β signaling pathway (*FBN1*, *SMAD3*, *TGFB2*, *TGFBR1*, and *TGFBR2*) and VSMC contraction pathway (*ACTA2*, *MYH11*, *MYLK*, and *PRKG1*). The TGF-β/*SMAD*3 pathway interacts with β-catenin in the canonical Wnt/β-catenin signaling pathway toward activation of TCF/LEF transcription factors (including *TCF7L2*) (Figure S6). Future studies should focus on understanding whether the effects observed in our experiments are dependent on its interaction with β-catenin[68] or other co-repressors or co-activators[69–71] or whether they may reflect the ability of *TCF7L2* to integrate signaling from other pathways, including TGF-β via *SMAD3*.[72]

Current treatment of aortic aneurysms involves surgical repair to reduce the risk of rupture, yet only a fraction of patients are eligible and those who are eligible are at high risk for post-surgery complications. Therapies for stabilization of aortic aneurysms have yet to prove efficacy in controlled clinical trials. Because of the involvement of this pathway in various diseases, present efforts in the drug development field are aimed at identifying inhibitors of the β-catenin-*TCF7L2* interactions[73] and the design of specific approaches targeting *TCF7L2* stability.[74] Our findings here highlight a potential path for *TCF7L2* as a target for intervention in individuals with TAA or for possible prevention in individuals at risk of TAA.

Data and code availability

TAA GWAS summary statistics from CHIP+MGI are available here: http://csg.sph.umich.edu/willer/public/TAA2021/. Analyses were performed by open-source software and cited in the material and methods.

Supplemental information

Supplemental information can be found online at https://doi.org/10.1016/j.ajhg.2021.06.016.

Acknowledgments

We thank all that contributed to the Cardiovascular Health Improvement Project and Michigan Genomics Initiative, including the financial support of the Frankel Cardiovascular Center (FCVC), Michigan Medicine, the Aikens Aortic Discovery Program of the FCVC, and the University of Michigan Medical School Central Biorepository for providing biospecimen management and distribution services. The Center for Statistical Genetics in the Department of Biostatistics at the School of Public Health provided genotype data curation, imputation, and management in support of this research (for MGI cohort). C.J.W. is supported by NIH grants R35-HL135824, R01-HL142023, and R01-HL109946. Y.E.C. is supported by NIH grants HL134569, HL109946, HL147527, and HL137214. J.Z. is supported by NIH grant HL138139. L.C. is supported by NIH grant HL122664. D.M. is supported by R01-HL109942-09, John Ritter Foundation, and Remembrin' Benjamin. S.M.D. is supported by IK2-CX001780. P.S.T. is supported by I01-BX003362. B.Y. is supported by K08-HL130614, R01-HL141891, and R01-HL151776. K.A.E. is supported by WL Gore and Marfan Foundation. B.N.W. is supported by NSF Graduate Research Fellowship (DGE 1256260). W.Z. is supported by NIH NHGRI under award number T32HG010464. HUNT-MI study, which comprises the genetic investigations of the HUNT Study, is a collaboration between investigators from the HUNT study and University of Michigan Medical School and the University of Michigan School of Public Health. The K.G. Jebsen Center for Genetic Epidemiology is financed by Stiftelsen Kristian Gerhard Jebsen; Faculty of Medicine

and Health Sciences, NTNU, Norwegian University of Science and Technology (NTNU), and Central Norway Regional Health Authority.

Declaration of interests

The spouse of C.J.W. is an employee of Regeneron. All other authors declare no competing interests.

Received: March 4, 2021
Accepted: June 18, 2021
Published: July 14, 2021

Web resources

DIAGRAM, https://diagram-consortium.org
ENCODE, https://www.encodeproject.org/
GTEx Portal, http://www.gtexportal.org/home/index.html
Promoter capture Hi-C, http://www.3div.kr/capture_hic

References

1. Hiratzka, L.F., Bakris, G.L., Beckman, J.A., Bersin, R.M., Carr, V.F., Casey, D.E., Jr., Eagle, K.A., Hermann, L.K., Isselbacher, E.M., Kazerooni, E.A., et al. (2010). 2010 ACCF/AHA/AATS/ACR/ASA/SCA/SCAI/SIR/STS/SVM guidelines for the diagnosis and management of patients with Thoracic Aortic Disease: a report of the American College of Cardiology Foundation/American Heart Association Task Force on Practice Guidelines, American Association for Thoracic Surgery, American College of Radiology, American Stroke Association, Society of Cardiovascular Anesthesiologists, Society for Cardiovascular Angiography and Interventions, Society of Interventional Radiology, Society of Thoracic Surgeons, and Society for Vascular Medicine. Circulation *121*, e266–e369.
2. Pinard, A., Jones, G.T., and Milewicz, D.M. (2019). Genetics of Thoracic and Abdominal Aortic Diseases. Circ. Res. *124*, 588–606.
3. Wolford, B.N., Hornsby, W.E., Guo, D., Zhou, W., Lin, M., Farhat, L., McNamara, J., Driscoll, A., Wu, X., Schmidt, E.M., et al. (2019). Clinical Implications of Identifying Pathogenic Variants in Individuals With Thoracic Aortic Dissection. Circ Genom Precis Med *12*, e002476.
4. Renard, M., Francis, C., Ghosh, R., Scott, A.F., Witmer, P.D., Adès, L.C., Andelfinger, G.U., Arnaud, P., Boileau, C., Callewaert, B.L., et al. (2018). Clinical Validity of Genes for Heritable Thoracic Aortic Aneurysm and Dissection. J. Am. Coll. Cardiol. *72*, 605–615.
5. Dietz, H.C., Cutting, G.R., Pyeritz, R.E., Maslen, C.L., Sakai, L.Y., Corson, G.M., Puffenberger, E.G., Hamosh, A., Nanthakumar, E.J., Curristin, S.M., et al. (1991). Marfan syndrome caused by a recurrent de novo missense mutation in the fibrillin gene. Nature *352*, 337–339.
6. Loeys, B.L., Schwarze, U., Holm, T., Callewaert, B.L., Thomas, G.H., Pannu, H., De Backer, J.F., Oswald, G.L., Symoens, S., Manouvrier, S., et al. (2006). Aneurysm syndromes caused by mutations in the TGF-beta receptor. N. Engl. J. Med. *355*, 788–798.
7. Rooprai, J., Boodhwani, M., Beauchesne, L., Chan, K.L., Dennie, C., Nagpal, S., Messika-Zeitoun, D., and Coutinho, T. (2019). Thoracic Aortic Aneurysm Growth in Bicuspid Aortic Valve Patients: Role of Aortic Stiffness and Pulsatile Hemodynamics. J. Am. Heart Assoc. *8*, e010885.
8. LeMaire, S.A., McDonald, M.L., Guo, D.C., Russell, L., Miller, C.C., 3rd, Johnson, R.J., Bekheirnia, M.R., Franco, L.M., Nguyen, M., Pyeritz, R.E., et al. (2011). Genome-wide association study identifies a susceptibility locus for thoracic aortic aneurysms and aortic dissections spanning FBN1 at 15q21.1. Nat. Genet. *43*, 996–1000.
9. Guo, D.C., Grove, M.L., Prakash, S.K., Eriksson, P., Hostetler, E.M., LeMaire, S.A., Body, S.C., Shalhub, S., Estrera, A.L., Safi, H.J., et al. (2016). Genetic Variants in LRP1 and ULK4 Are Associated with Acute Aortic Dissections. Am. J. Hum. Genet. *99*, 762–769.
10. Fritsche, L.G., Gruber, S.B., Wu, Z., Schmidt, E.M., Zawistowski, M., Moser, S.E., Blanc, V.M., Brummett, C.M., Kheterpal, S., Abecasis, G.R., and Mukherjee, B. (2018). Association of Polygenic Risk Scores for Multiple Cancers in a Phenome-wide Study: Results from The Michigan Genomics Initiative. Am. J. Hum. Genet. *102*, 1048–1061.
11. Jun, G., Flickinger, M., Hetrick, K.N., Romm, J.M., Doheny, K.F., Abecasis, G.R., Boehnke, M., and Kang, H.M. (2012). Detecting and estimating contamination of human DNA samples in sequencing and array-based genotype data. Am. J. Hum. Genet. *91*, 839–848.
12. Taliun, D., Chothani, S.P., Schönherr, S., Forer, L., Boehnke, M., Abecasis, G.R., and Wang, C. (2017). LASER server: ancestry tracing with genotypes or sequence reads. Bioinformatics *33*, 2056–2058.
13. Manichaikul, A., Mychaleckyj, J.C., Rich, S.S., Daly, K., Sale, M., and Chen, W.M. (2010). Robust relationship inference in genome-wide association studies. Bioinformatics *26*, 2867–2873.
14. McCarthy, S., Das, S., Kretzschmar, W., Delaneau, O., Wood, A.R., Teumer, A., Kang, H.M., Fuchsberger, C., Danecek, P., Sharp, K., et al. (2016). A reference panel of 64,976 haplotypes for genotype imputation. Nat. Genet. *48*, 1279–1283.
15. Das, S., Forer, L., Schönherr, S., Sidore, C., Locke, A.E., Kwong, A., Vrieze, S.I., Chew, E.Y., Levy, S., McGue, M., et al. (2016). Next-generation genotype imputation service and methods. Nat. Genet. *48*, 1284–1287.
16. Yang, B., Zhou, W., Jiao, J., Nielsen, J.B., Mathis, M.R., Heydarpour, M., Lettre, G., Folkersen, L., Prakash, S., Schurmann, C., et al. (2017). Protein-altering and regulatory genetic variants near GATA4 implicated in bicuspid aortic valve. Nat. Commun. *8*, 15481.
17. Pasta, S., Rinaudo, A., Luca, A., Pilato, M., Scardulla, C., Gleason, T.G., and Vorp, D.A. (2013). Difference in hemodynamic and wall stress of ascending thoracic aortic aneurysms with bicuspid and tricuspid aortic valve. J. Biomech. *46*, 1729–1738.
18. Zhou, W., Nielsen, J.B., Fritsche, L.G., Dey, R., Gabrielsen, M.E., Wolford, B.N., LeFaive, J., VandeHaar, P., Gagliano, S.A., Gifford, A., et al. (2018). Efficiently controlling for case-control imbalance and sample relatedness in large-scale genetic association studies. Nat. Genet. *50*, 1335–1341.
19. Hunter-Zinck, H., Shi, Y., Li, M., Gorman, B.R., Ji, S.G., Sun, N., Webster, T., Liem, A., Hsieh, P., Devineni, P., et al. (2020). Genotyping Array Design and Data Quality Control in the Million Veteran Program. Am. J. Hum. Genet. *106*, 535–548.
20. Fang, H., Hui, Q., Lynch, J., Honerlaw, J., Assimes, T.L., Huang, J., Vujkovic, M., Damrauer, S.M., Pyarajan, S., Gaziano, J.M., et al. (2019). Harmonizing Genetic Ancestry and Self-identified Race/Ethnicity in Genome-wide Association Studies. Am. J. Hum. Genet. *105*, 763–772.

21. Krokstad, S., Langhammer, A., Hveem, K., Holmen, T.L., Midthjell, K., Stene, T.R., Bratberg, G., Heggland, J., and Holmen, J. (2013). Cohort Profile: the HUNT Study, Norway. Int. J. Epidemiol. *42*, 968–977.
22. Nielsen, J.B., Thorolfsdottir, R.B., Fritsche, L.G., Zhou, W., Skov, M.W., Graham, S.E., Herron, T.J., McCarthy, S., Schmidt, E.M., Sveinbjornsson, G., et al. (2018). Biobank-driven genomic discovery yields new insight into atrial fibrillation biology. Nat. Genet. *50*, 1234–1239.
23. Sudlow, C., Gallacher, J., Allen, N., Beral, V., Burton, P., Danesh, J., Downey, P., Elliott, P., Green, J., Landray, M., et al. (2015). UK biobank: an open access resource for identifying the causes of a wide range of complex diseases of middle and old age. PLoS Med. *12*, e1001779.
24. Willer, C.J., Li, Y., and Abecasis, G.R. (2010). METAL: fast and efficient meta-analysis of genomewide association scans. Bioinformatics *26*, 2190–2191.
25. Jung, I., Schmitt, A., Diao, Y., Lee, A.J., Liu, T., Yang, D., Tan, C., Eom, J., Chan, M., Chee, S., et al. (2019). A compendium of promoter-centered long-range chromatin interactions in the human genome. Nat. Genet. *51*, 1442–1449.
26. Yang, J., Lee, S.H., Goddard, M.E., and Visscher, P.M. (2011). GCTA: a tool for genome-wide complex trait analysis. Am. J. Hum. Genet. *88*, 76–82.
27. Giambartolomei, C., Vukcevic, D., Schadt, E.E., Franke, L., Hingorani, A.D., Wallace, C., and Plagnol, V. (2014). Bayesian test for colocalisation between pairs of genetic association studies using summary statistics. PLoS Genet. *10*, e1004383.
28. Barbeira, A.N., Dickinson, S.P., Bonazzola, R., Zheng, J., Wheeler, H.E., Torres, J.M., Torstenson, E.S., Shah, K.P., Garcia, T., Edwards, T.L., et al. (2018). Exploring the phenotypic consequences of tissue specific gene expression variation inferred from GWAS summary statistics. Nat. Commun. *9*, 1825.
29. GTEx Consortium (2020). The GTEx Consortium atlas of genetic regulatory effects across human tissues. Science *369*, 1318–1330.
30. Benner, C., Spencer, C.C., Havulinna, A.S., Salomaa, V., Ripatti, S., and Pirinen, M. (2016). FINEMAP: efficient variable selection using summary data from genome-wide association studies. Bioinformatics *32*, 1493–1501.
31. Purcell, S., Neale, B., Todd-Brown, K., Thomas, L., Ferreira, M.A., Bender, D., Maller, J., Sklar, P., de Bakker, P.I., Daly, M.J., and Sham, P.C. (2007). PLINK: a tool set for whole-genome association and population-based linkage analyses. Am. J. Hum. Genet. *81*, 559–575.
32. Boyle, A.P., Hong, E.L., Hariharan, M., Cheng, Y., Schaub, M.A., Kasowski, M., Karczewski, K.J., Park, J., Hitz, B.C., Weng, S., et al. (2012). Annotation of functional variation in personal genomes using RegulomeDB. Genome Res. *22*, 1790–1797.
33. Snyder, M.P., Gingeras, T.R., Moore, J.E., Weng, Z., Gerstein, M.B., Ren, B., Hardison, R.C., Stamatoyannopoulos, J.A., Graveley, B.R., Feingold, E.A., et al. (2020). Perspectives on ENCODE. Nature *583*, 693–698.
34. Bulik-Sullivan, B.K., Loh, P.R., Finucane, H.K., Ripke, S., Yang, J., Patterson, N., Daly, M.J., Price, A.L., Neale, B.M.; and Schizophrenia Working Group of the Psychiatric Genomics Consortium (2015). LD Score regression distinguishes confounding from polygenicity in genome-wide association studies. Nat. Genet. *47*, 291–295.
35. Zheng, J., Erzurumluoglu, A.M., Elsworth, B.L., Kemp, J.P., Howe, L., Haycock, P.C., Hemani, G., Tansey, K., Laurin, C., Pourcain, B.S., et al. (2017). LD Hub: a centralized database and web interface to perform LD score regression that maximizes the potential of summary level GWAS data for SNP heritability and genetic correlation analysis. Bioinformatics *33*, 272–279.
36. Tetsu, O., and McCormick, F. (1999). Beta-catenin regulates expression of cyclin D1 in colon carcinoma cells. Nature *398*, 422–426.
37. Lu, H., Sun, J., Liang, W., Chang, Z., Rom, O., Zhao, Y., Zhao, G., Xiong, W., Wang, H., Zhu, T., et al. (2020). Cyclodextrin Prevents Abdominal Aortic Aneurysm via Activation of Vascular Smooth Muscle Cell Transcription Factor EB. Circulation *142*, 483–498.
38. Kälsch, H., Lehmann, N., Möhlenkamp, S., Becker, A., Moebus, S., Schmermund, A., Stang, A., Mahabadi, A.A., Mann, K., Jöckel, K.H., et al. (2013). Body-surface adjusted aortic reference diameters for improved identification of patients with thoracic aortic aneurysms: results from the population-based Heinz Nixdorf Recall study. Int. J. Cardiol. *163*, 72–78.
39. Klarin, D., Verma, S.S., Judy, R., Dikilitas, O., Wolford, B.N., Paranjpe, I., Levin, M.G., Pan, C., Tcheandjieu, C., Spin, J.M., et al. (2020). Genetic Architecture of Abdominal Aortic Aneurysm in the Million Veteran Program. Circulation *142*, 1633–1646.
40. Bakker, M.K., van der Spek, R.A.A., van Rheenen, W., Morel, S., Bourcier, R., Hostettler, I.C., Alg, V.S., van Eijk, K.R., Koido, M., Akiyama, M., et al. (2020). Genome-wide association study of intracranial aneurysms identifies 17 risk loci and genetic overlap with clinical risk factors. Nat. Genet. *52*, 1303–1313.
41. Grant, S.F., Thorleifsson, G., Reynisdottir, I., Benediktsson, R., Manolescu, A., Sainz, J., Helgason, A., Stefansson, H., Emilsson, V., Helgadottir, A., et al. (2006). Variant of transcription factor 7-like 2 (TCF7L2) gene confers risk of type 2 diabetes. Nat. Genet. *38*, 320–323.
42. Gloyn, A.L., Braun, M., and Rorsman, P. (2009). Type 2 diabetes susceptibility gene TCF7L2 and its role in beta-cell function. Diabetes *58*, 800–802.
43. Mahajan, A., Taliun, D., Thurner, M., Robertson, N.R., Torres, J.M., Rayner, N.W., Payne, A.J., Steinthorsdottir, V., Scott, R.A., Grarup, N., et al. (2018). Fine-mapping type 2 diabetes loci to single-variant resolution using high-density imputation and islet-specific epigenome maps. Nat. Genet. *50*, 1505–1513.
44. Hormozdiari, F., Kostem, E., Kang, E.Y., Pasaniuc, B., and Eskin, E. (2014). Identifying causal variants at loci with multiple signals of association. Genetics *198*, 497–508.
45. He, R., Guo, D.C., Estrera, A.L., Safi, H.J., Huynh, T.T., Yin, Z., Cao, S.N., Lin, J., Kurian, T., Buja, L.M., et al. (2006). Characterization of the inflammatory and apoptotic cells in the aortas of patients with ascending thoracic aortic aneurysms and dissections. J. Thorac. Cardiovasc. Surg. *131*, 671–678.
46. Durdu, S., Deniz, G.C., Balci, D., Zaim, C., Dogan, A., Can, A., Akcali, K.C., and Akar, A.R. (2012). Apoptotic vascular smooth muscle cell depletion via BCL2 family of proteins in human ascending aortic aneurysm and dissection. Cardiovasc. Ther. *30*, 308–316.
47. Srivastava, R., Rolyan, H., Xie, Y., Li, N., Bhat, N., Hong, L., Esteghamat, F., Adeniran, A., Geirsson, A., Zhang, J., et al. (2019). TCF7L2 (Transcription Factor 7-Like 2) Regulation of GATA6 (GATA-Binding Protein 6)-Dependent and -Independent Vascular Smooth Muscle Cell Plasticity and Intimal Hyperplasia. Arterioscler. Thromb. Vasc. Biol. *39*, 250–262.
48. Srivastava, R., Zhang, J., Go, G.W., Narayanan, A., Nottoli, T.P., and Mani, A. (2015). Impaired LRP6-TCF7L2 Activity

Enhances Smooth Muscle Cell Plasticity and Causes Coronary Artery Disease. Cell Rep. *13*, 746–759.

49. Wang, X., Adhikari, N., Li, Q., and Hall, J.L. (2004). LDL receptor-related protein LRP6 regulates proliferation and survival through the Wnt cascade in vascular smooth muscle cells. Am. J. Physiol. Heart Circ. Physiol. *287*, H2376–H2383.
50. Liu, X., Huang, Y., Zhang, Y., Li, X., Liu, C., Huang, S., Xu, D., Wu, Y., and Liu, X. (2016). T-cell factor (TCF/LEF1) binding elements (TBEs) of FasL (Fas ligand or CD95 ligand) bind and cluster Fas (CD95) and form complexes with the TCF-4 and b-catenin transcription factors in vitro and in vivo which result in triggering cell death and/or cell activation. Cell. Mol. Neurobiol. *36*, 1001–1013.
51. Ma, B., Zhong, L., van Blitterswijk, C.A., Post, J.N., and Karperien, M. (2013). T cell factor 4 is a pro-catabolic and apoptotic factor in human articular chondrocytes by potentiating nuclear factor κB signaling. J. Biol. Chem. *288*, 17552–17558.
52. Li, H., Ma, Y., Chen, B., and Shi, J. (2018). miR-182 enhances acute kidney injury by promoting apoptosis involving the targeting and regulation of TCF7L2/Wnt/β-catenins pathway. Eur. J. Pharmacol. *831*, 20–27.
53. Zhou, Y., Zhang, E., Berggreen, C., Jing, X., Osmark, P., Lang, S., Cilio, C.M., Göransson, O., Groop, L., Renström, E., and Hansson, O. (2012). Survival of pancreatic beta cells is partly controlled by a TCF7L2-p53-p53INP1-dependent pathway. Hum. Mol. Genet. *21*, 196–207.
54. Henderson, E.L., Geng, Y.J., Sukhova, G.K., Whittemore, A.D., Knox, J., and Libby, P. (1999). Death of smooth muscle cells and expression of mediators of apoptosis by T lymphocytes in human abdominal aortic aneurysms. Circulation *99*, 96–104.
55. Viñuela, A., Varshney, A., van de Bunt, M., Prasad, R.B., Asplund, O., Bennett, A., Boehnke, M., Brown, A.A., Erdos, M.R., Fadista, J., et al. (2020). Genetic variant effects on gene expression in human pancreatic islets and their implications for T2D. Nat. Commun. *11*, 4912.
56. Patel, K., Zafar, M.A., Ziganshin, B.A., and Elefteriades, J.A. (2018). Diabetes Mellitus: Is It Protective against Aneurysm? A Narrative Review. Cardiology *141*, 107–122.
57. Takagi, H., Umemoto, T.; and ALICE (All-Literature Investigation of Cardiovascular Evidence) Group (2017). Negative Association of Diabetes With Thoracic Aortic Dissection and Aneurysm. Angiology *68*, 216–224.
58. Raffort, J., Lareyre, F., Clément, M., Hassen-Khodja, R., Chinetti, G., and Mallat, Z. (2018). Diabetes and aortic aneurysm: current state of the art. Cardiovasc. Res. *114*, 1702–1713.
59. Yi, F., Brubaker, P.L., and Jin, T. (2005). TCF-4 mediates cell type-specific regulation of proglucagon gene expression by beta-catenin and glycogen synthase kinase-3beta. J. Biol. Chem. *280*, 1457–1464.
60. Komiya, Y., and Habas, R. (2008). Wnt signal transduction pathways. Organogenesis *4*, 68–75.
61. Ng, L.F., Kaur, P., Bunnag, N., Suresh, J., Sung, I.C.H., Tan, Q.H., Gruber, J., and Tolwinski, N.S. (2019). WNT Signaling in Disease. Cells *8*, E826.
62. Facchinello, N., Tarifeño-Saldivia, E., Grisan, E., Schiavone, M., Peron, M., Mongera, A., Ek, O., Schmitner, N., Meyer, D., Peers, B., et al. (2017). Tcf7l2 plays pleiotropic roles in the control of glucose homeostasis, pancreas morphology, vascularization and regeneration. Sci. Rep. *7*, 9605.
63. Wang, S., Huang, H., Xiang, H., Gu, B., Li, W., Chen, L., and Zhang, M. (2019). Wnt Signaling Modulates Routes of Retinoic Acid-Induced Differentiation of Embryonic Stem Cells. Stem Cells Dev. *28*, 1334–1345.
64. Corada, M., Nyqvist, D., Orsenigo, F., Caprini, A., Giampietro, C., Taketo, M.M., Iruela-Arispe, M.L., Adams, R.H., and Dejana, E. (2010). The Wnt/beta-catenin pathway modulates vascular remodeling and specification by upregulating Dll4/Notch signaling. Dev. Cell *18*, 938–949.
65. Wang, X., Xiao, Y., Mou, Y., Zhao, Y., Blankesteijn, W.M., and Hall, J.L. (2002). A role for the beta-catenin/T-cell factor signaling cascade in vascular remodeling. Circ. Res. *90*, 340–347.
66. Krishna, S.M., Seto, S.W., Jose, R.J., Li, J., Morton, S.K., Biros, E., Wang, Y., Nsengiyumva, V., Lindeman, J.H., Loots, G.G., et al. (2017). Wnt Signaling Pathway Inhibitor Sclerostin Inhibits Angiotensin II-Induced Aortic Aneurysm and Atherosclerosis. Arterioscler. Thromb. Vasc. Biol. *37*, 553–566.
67. Kostina, A., Bjork, H., Ignatieva, E., Irtyuga, O., Uspensky, V., Semenova, D., Maleki, S., Tomilin, A., Moiseeva, O., Franco-Cereceda, A., et al. (2018). Notch, BMP and WNT/β-catenin network is impaired in endothelial cells of the patients with thoracic aortic aneurysm. Atheroscler. Suppl. *35*, e6–e13.
68. Graham, T.A., Ferkey, D.M., Mao, F., Kimelman, D., and Xu, W. (2001). Tcf4 can specifically recognize beta-catenin using alternative conformations. Nat. Struct. Biol. *8*, 1048–1052.
69. Valenta, T., Lukas, J., and Korinek, V. (2003). HMG box transcription factor TCF-4's interaction with CtBP1 controls the expression of the Wnt target Axin2/Conductin in human embryonic kidney cells. Nucleic Acids Res. *31*, 2369–2380.
70. Brantjes, H., Roose, J., van De Wetering, M., and Clevers, H. (2001). All Tcf HMG box transcription factors interact with Groucho-related co-repressors. Nucleic Acids Res. *29*, 1410–1419.
71. Hecht, A., and Stemmler, M.P. (2003). Identification of a promoter-specific transcriptional activation domain at the C terminus of the Wnt effector protein T-cell factor 4. J. Biol. Chem. *278*, 3776–3785.
72. Labbé, E., Letamendia, A., and Attisano, L. (2000). Association of Smads with lymphoid enhancer binding factor 1/T cell-specific factor mediates cooperative signaling by the transforming growth factor-beta and wnt pathways. Proc. Natl. Acad. Sci. USA *97*, 8358–8363.
73. Tian, W., Han, X., Yan, M., Xu, Y., Duggineni, S., Lin, N., Luo, G., Li, Y.M., Han, X., Huang, Z., and An, J. (2012). Structure-based discovery of a novel inhibitor targeting the β-catenin/Tcf4 interaction. Biochemistry *51*, 724–731.
74. Zhang, H., Rong, X., Wang, C., Liu, Y., Lu, L., Li, Y., Zhao, C., and Zhou, J. (2020). VBP1 modulates Wnt/β-catenin signaling by mediating the stability of the transcription factors TCF/LEFs. J. Biol. Chem. *295*, 16826–16839.

The American Journal of Human Genetics, Volume *108*

Supplemental Data

Regulatory variants in *TCF7L2* are associated with thoracic aortic aneurysm

Tanmoy Roychowdhury, Haocheng Lu, Whitney E. Hornsby, Bradley Crone, Gao T. Wang, Dong-chuan Guo, Anoop K. Sendamarai, Poornima Devineni, Maoxuan Lin, Wei Zhou, Sarah E. Graham, Brooke N. Wolford, Ida Surakka, Zhenguo Wang, Lin Chang, Jifeng Zhang, Michael Mathis, Chad M. Brummett, Tori L. Melendez, Michael J. Shea, Karen Meekyong Kim, G. Michael Deeb, Himanshu J. Patel, Jonathan Eliason, Kim A. Eagle, Bo Yang, Santhi K. Ganesh, Ben Brumpton, Bjørn Olav Åsvold, Anne Heidi Skogholt, Kristian Hveem, VA Million Veteran Program, Saiju Pyarajan, Derek Klarin, Philip S. Tsao, Scott M. Damrauer, Suzanne M. Leal, Dianna M. Milewicz, Y. Eugene Chen, Minerva T. Garcia-Barrio, and Cristen J. Willer

Supplementary Information

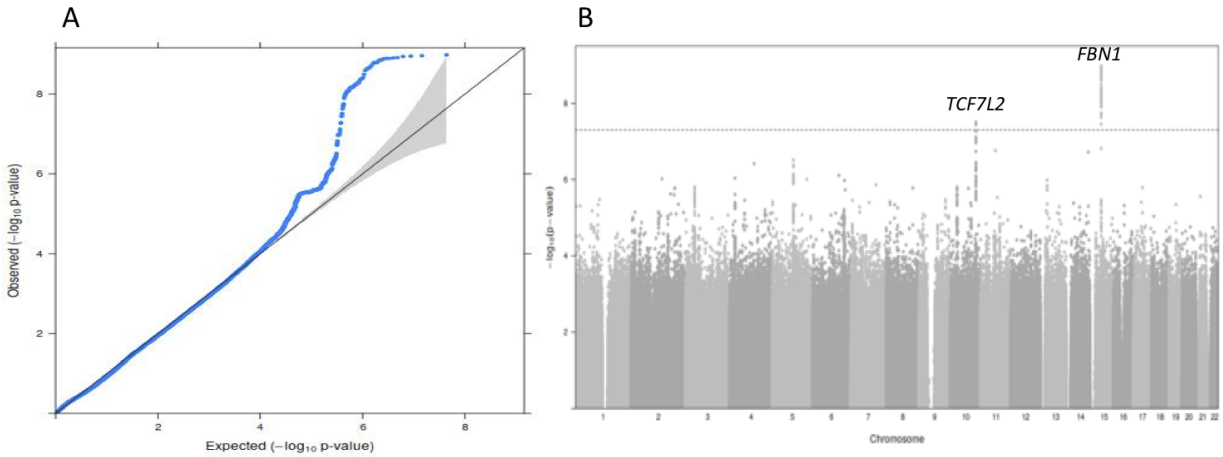

Figure S1: GWAS of TAA in CHIP/MGI. A) QQ plot. **B)** Manhattan plot.

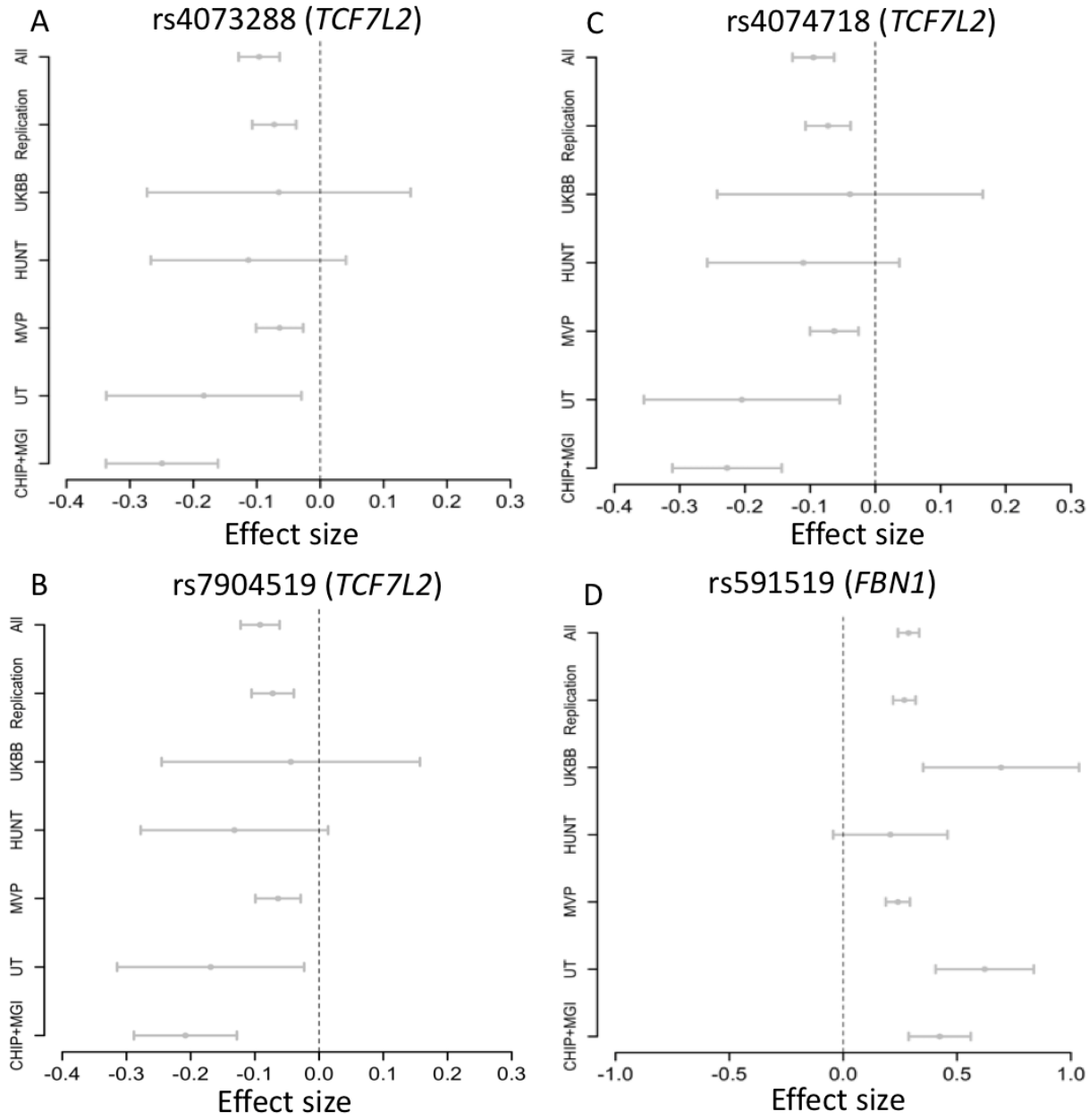

Figure S2: Effect sizes in discovery and replication cohorts. Effect size estimation for 3 variants in *TCF7L2* locus **(A-C)** and *FBN1* index variant **(D)** in individual cohorts, replication (UT+MVP+HUNT+UKBB), All (CHIP+MGI+Replication).

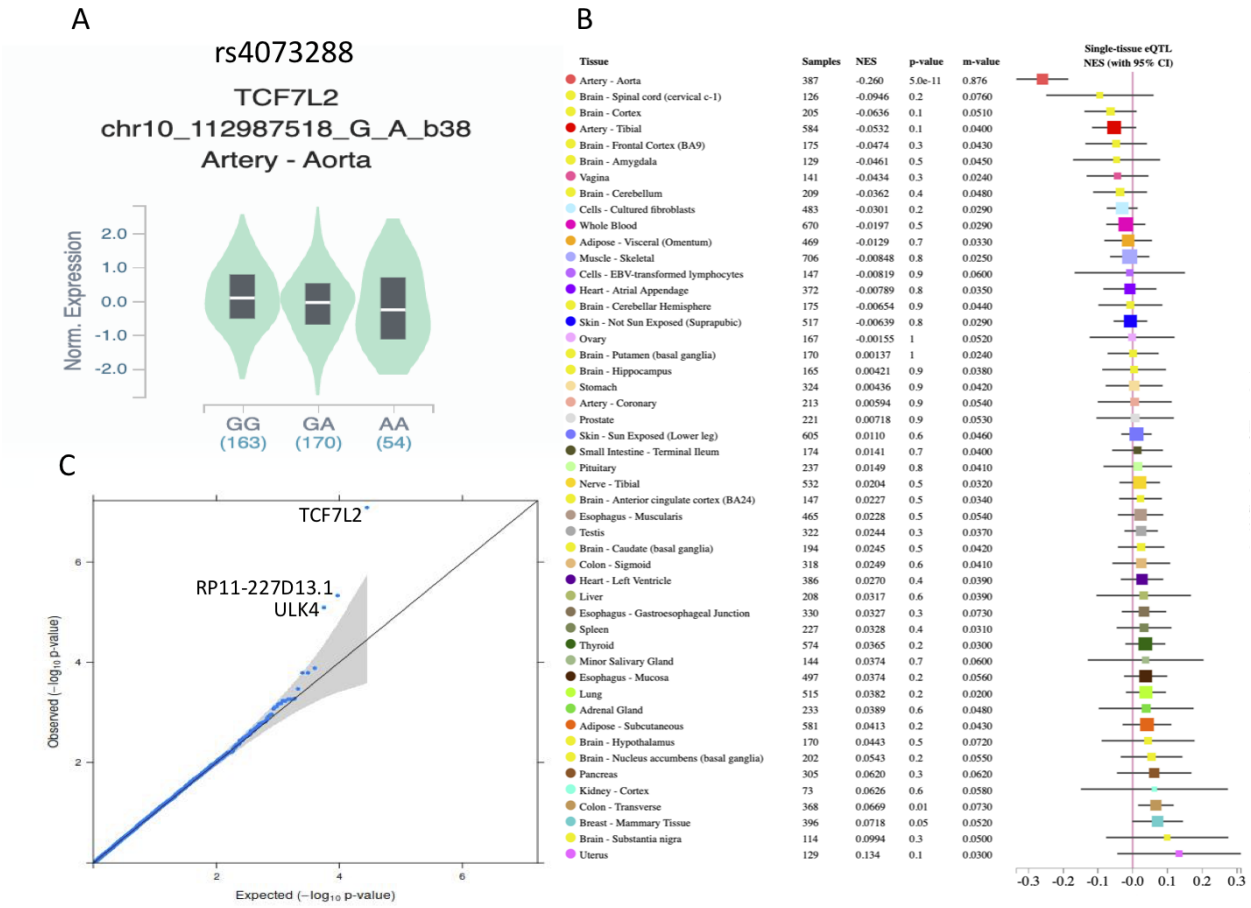

Figure S3: **eQTL**. **A)** rs4073288 is an aortic eQTL of *TCF7L2* from GTEx V8. TAA risk allele G is associated with higher expression of gene. **B)** This eQTL is only significant in aorta in GTEx V8. **C)** QQ plot of TWAS using SPrediXcan.

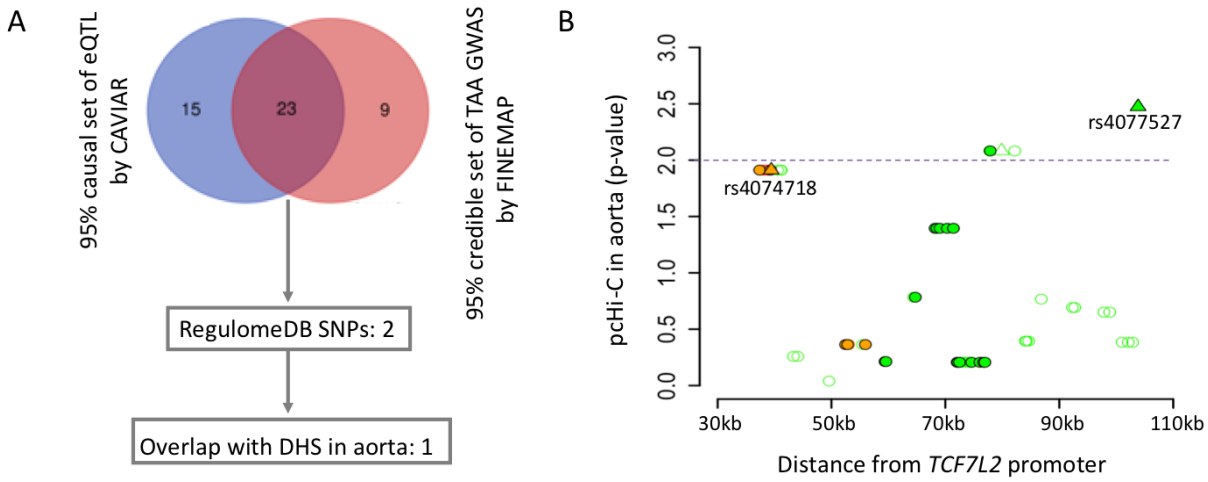

Figure S4: Fine-mapping of *TCF7L2* loci. A) 23 variants were found to be common between the credible sets of TAA GWAS and eQTL (rs4073980, rs4074720, rs4074718, rs10885402, rs6585197, rs6585199, rs6585200, rs6585201, rs7904519, rs7918599, rs10885406, rs11196190, rs7899529, rs11196191, rs10787472, rs10787473, rs12258200, rs11196193, rs4309084, rs4128598, rs4128597, rs7907610, rs4077527) **B)** Promoter capture Hi-C -log10(p-values) of variants that are in LD > 0.4 with TAA index variant rs4073288. Solid shapes are 23 variants mentioned in A. Triangles represent variants prioritized by regulomeDB. The dotted line is the significance threshold as suggested by Jung et al. [PMID: 31501517].

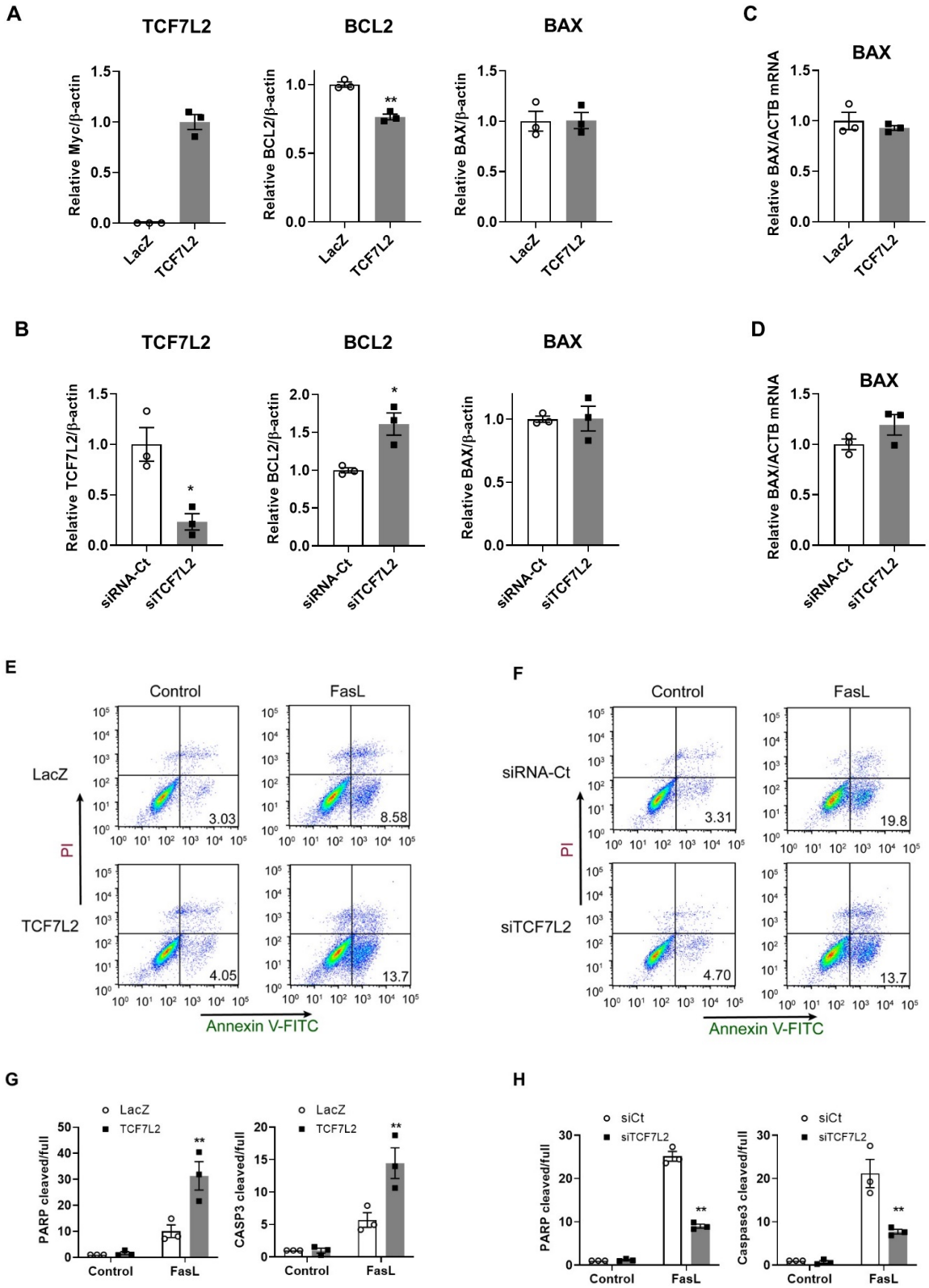
A
TCF7L2
BCL2
BAX
Relative Myc/β-actin
Relative BCL2/β-actin
Relative BAX/β-actin
LacZ
TCF7L2
C
BAX
Relative BAX/ACTB mRNA
B
TCF7L2
BCL2
BAX
Relative TCF7L2/β-actin
Relative BCL2/β-actin
Relative BAX/β-actin
siRNA-Ct
siTCF7L2
D
BAX
Relative BAX/ACTB mRNA
E
Control
FasL
LacZ
TCF7L2
PI
Annexin V-FITC
3.03
8.58
4.05
13.7
F
Control
FasL
siRNA-Ct
siTCF7L2
PI
Annexin V-FITC
3.31
19.8
4.70
13.7
G
LacZ
TCF7L2
PARP cleaved/full
CASP3 cleaved/full
Control
FasL
H
siCt
siTCF7L2
PARP cleaved/full
Caspase3 cleaved/full
Control
FasL

Figure S5. ***TCF7L2*** **expression is associated with vascular smooth muscle cell apoptosis** ***in vitro***: A and B, densitometry of 3 independent Western blots as in Figure 3 A and B. **A)** Overexpression of *TCF7L2* showing significant downregulation of *BCL2*, P=0.0011. Densitometry for Myc-TCF7L2 shows reproducibility among the three independent experiments. **B)** Knockdown of *TCF7L2* (*TCF7L2*, P=0.0145) showing significant upregulation of *BCL2*, P=0.0154. **C)** upregulation of *TCF7L2* or **D)** siRNA-mediated knockdown of *TCF7L2* does not change expression of *BAX* mRNA. Representative graphs of Annexin-V by FACS analysis in response to **E)** upregulation or **F)** knockdown of TCF7L2, respectively (n=3; representative of 3 independent experiments). **G and H**, Densitometry of 3 independent Western blots as in Figure 3 F and H. Data are expressed as the ratio between either cleaved PARP or cleaved caspase-3 and its corresponding full length counterpart. **G)** Overexpression of *TCF7L2* combined with FasL treatment: PARP, P=0.0021; Capase3, P=0.0031. **H)** Downregulation of *TCF7L2* combined with FasL treatment: PARP, P<0.0001; Capase3, P=0.0009.

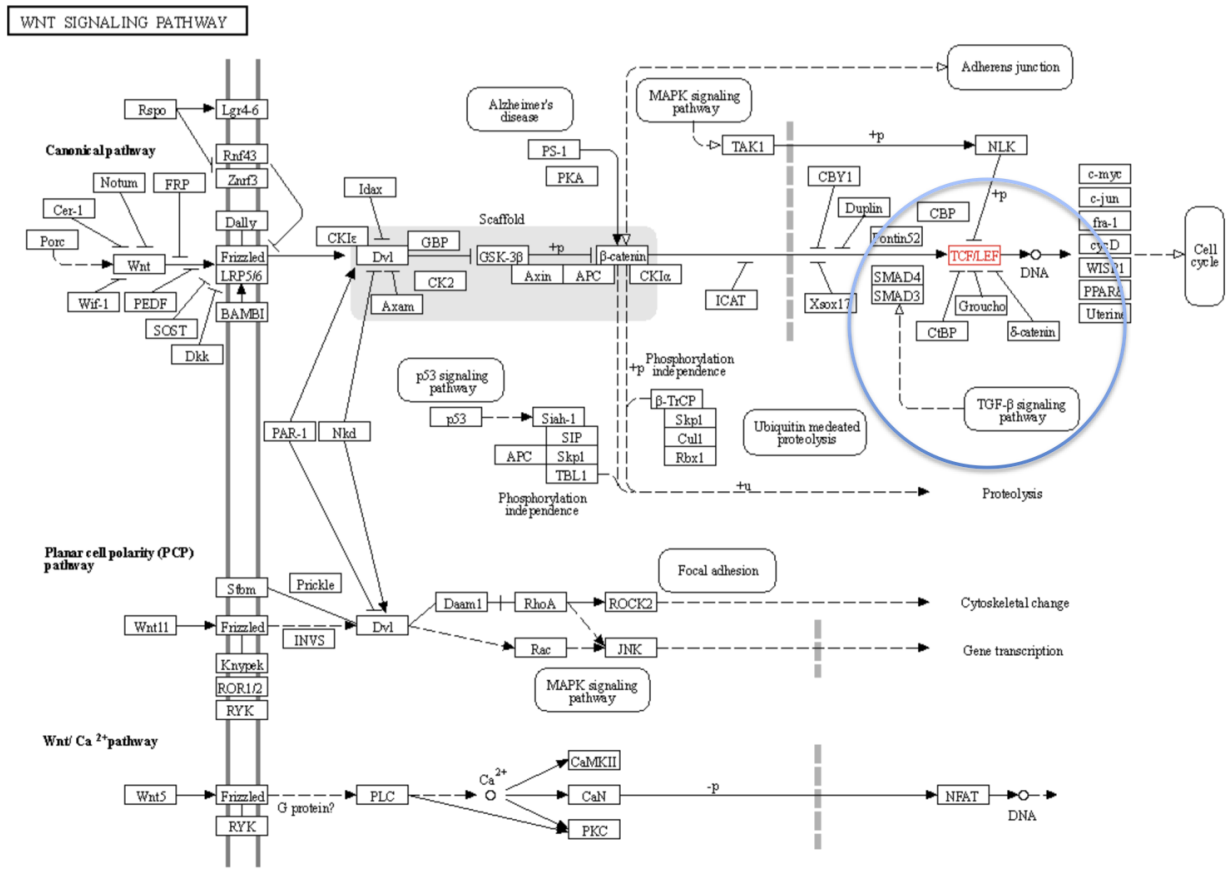

Figure S6: Wnt signaling pathway from KEGG.

Table S1: Characteristics of discovery and replication cohorts

CHIP+MGI	Cases	Controls
Male	71.3%	74%
Median birth year	1948	1954
Present or past smoking*	10.2%	10%
UT**		
Male	65.4%	NA
Median Age	65	NA
Present or past smoking	61.4%	NA
MVP		
Male	97.9%	90.6%
Median age	73	69
HUNT		
Male	64.4%	46.9%
Median birth year	1942	1951
Present or past smoking	64.4%	57.9%
UKBB		
Male	68.1%	68.6%
Median birth year	1945	1945
Present or past smoking	67.7%	64.1%

*Smoking information in MGI was obtained by ICD codes.

**UT data was obtained from supplementary table 1 of LeMaire et al. (https://www.nature.com/articles/ng.934#MOESM20)

Table S2: Codes used for case-control selection in MVP cohort.

TAA CONTROLS	
(cannot have any of the following codes, ever)	
441	Dissection of aorta, unspecified site
441.01	Dissection of aorta, thoracic
441.02	Dissection of aorta, abdominal
441.03	Dissection of aorta, thoracoabdominal
441.1	Thoracic aneurysm, ruptured
441.2	Thoracic aneurysm without mention of rupture
441.5	Aortic aneurysm of unspecified site, ruptured
441.6	Thoracoabdominal aneurysm, ruptured
441.7	Thoracoabdominal aneurysm, without mention of rupture
441.9	Aortic aneurysm of unspecified site without mention of rupture
I71.00	Dissection of unspecified site of aorta
I71.01	Dissection of thoracic aorta
I71.02	Dissection of abdominal aorta
I71.03	Dissection of thoracoabdominal aorta
I71.1	Thoracic aortic aneurysm, ruptured

I71.2	Thoracic aortic aneurysm, without rupture
I71.5	Thoracoabdominal aortic aneurysm, ruptured
I71.6	Thoracoabdominal aortic aneurysm, without rupture
I71.8	Aortic aneurysm of unspecified site, ruptured
I71.9	Aortic aneurysm of unspecified site, without rupture
746.4	Congenital insufficiency of aortic valve
Q23.1	Congenital insufficiency of aortic valve

controls cannot have any of the *_REPAIR codes (ASC_REPAIR, ARCH_REPEAR, DESC_REPAIR, ANY_REPAIR)
controls must also have 2 visits to the VA in each of the two years prior to MVP enrollment

ASC_REPAIR (ascending)
defined as having any of the following CPT codes:

33860	Ascending aortic replacement with valve resuspension when performed
33861	Ascending aorta graft, with cardiopulmonary bypass, with or without valve suspension; with coronary reconstruction
33858	Ascending aortic replacement with valve resuspension when performed (dissection)
33859	Ascending aortic replacement with valve resuspension when performed (non-dissection)
33863	Root replacement (Bentall)
33864	Valve sparing root reconstruction (David)
02QX0ZZ	Repair Thoracic Aorta, Ascending/Arch, Open Approach
02QX3ZZ	Repair Thoracic Aorta, Ascending/Arch, Percutaneous Approach
02QX4ZZ	Repair Thoracic Aorta, Ascending/Arch, Percutaneous Endoscopic Approach
02RX07Z	Replacement of Thoracic Aorta, Ascending/Arch with Autologous Tissue Substitute, Open Approach
02RX08Z	Replacement of Thoracic Aorta, Ascending/Arch with Zooplastic Tissue, Open Approach
02RX0JZ	Replacement of Thoracic Aorta, Ascending/Arch with Synthetic Substitute, Open Approach
02RX0KZ	Replacement of Thoracic Aorta, Ascending/Arch with Nonautologous Tissue Substitute, Open Approach
02RX47Z	Replacement of Thoracic Aorta, Ascending/Arch with Autologous Tissue Substitute, Percutaneous Endoscopic Approach
02RX48Z	Replacement of Thoracic Aorta, Ascending/Arch with Zooplastic Tissue, Percutaneous Endoscopic Approach
02RX4JZ	Replacement of Thoracic Aorta, Ascending/Arch with Synthetic Substitute, Percutaneous Endoscopic Approach
02RX4KZ	Replacement of Thoracic Aorta, Ascending/Arch with Nonautologous Tissue Substitute, Percutaneous Endoscopic Approach

02VX0DZ	Restriction of Thoracic Aorta, Ascending/Arch with Intraluminal Device, Open Approach
02VX0EZ	Restriction of Thoracic Aorta, Ascending/Arch with Branched or Fenestrated Intraluminal Device, One or Two Arteries, Open Approach
02VX0FZ	Restriction of Thoracic Aorta, Ascending/Arch with Branched or Fenestrated Intraluminal Device, Three or More Arteries, Open Approach
02VX0ZZ	Restriction of Thoracic Aorta, Ascending/Arch, Open Approach
02VX3DZ	Restriction of Thoracic Aorta, Ascending/Arch with Intraluminal Device, Percutaneous Approach
02VX3EZ	Restriction of Thoracic Aorta, Ascending/Arch with Branched or Fenestrated Intraluminal Device, One or Two Arteries, Percutaneous Approach
02VX3FZ	Restriction of Thoracic Aorta, Ascending/Arch with Branched or Fenestrated Intraluminal Device, Three or More Arteries, Percutaneous Approach
02VX3ZZ	Restriction of Thoracic Aorta, Ascending/Arch, Percutaneous Approach

ARCH_REPAIR

defined as having any of the following CPT codes:

33866	Hemiarch reconstruction
33871	Extended arch procedures (more than hemiarch)
33870	Transverse arch graft

DESC_REPAIR (descending)

defined as having any of the following CPT codes:

33877	Repair TAAA with graft, with or without bypass
33875	Repair TAA with graft, with or without bypass
33880	TEVAR (Zone 2)
33881	TEVAR (not Zone 2)
33877	Repair of thoracoadbominal aortic aneurysm with graft
02QW0ZZ	Repair Thoracic Aorta, Descending, Open Approach
02QW3ZZ	Repair Thoracic Aorta, Descending, Percutaneous Approach
02QW4ZZ	Repair Thoracic Aorta, Descending, Percutaneous Endoscopic Approach
02RW07Z	Replacement of Thoracic Aorta, Descending with Autologous Tissue Substitute, Open Approach
02RW08Z	Replacement of Thoracic Aorta, Descending with Zooplastic Tissue, Open Approach
02RW0JZ	Replacement of Thoracic Aorta, Descending with Synthetic Substitute, Open Approach
02RW0KZ	Replacement of Thoracic Aorta, Descending with Nonautologous Tissue Substitute, Open Approach
02RW47Z	Replacement of Thoracic Aorta, Descending with Autologous Tissue Substitute, Percutaneous Endoscopic Approach
02RW48Z	Replacement of Thoracic Aorta, Descending with Zooplastic Tissue, Percutaneous Endoscopic Approach

02RW4JZ	Replacement of Thoracic Aorta, Descending with Synthetic Substitute, Percutaneous Endoscopic Approach
02RW4KZ	Replacement of Thoracic Aorta, Descending with Nonautologous Tissue Substitute, Percutaneous Endoscopic Approach
02VW3DZ	Restriction of Thoracic Aorta, Descending with Intraluminal Device, Percutaneous Approach
02VW0DZ	Restriction of Thoracic Aorta, Descending with Intraluminal Device, Open Approach
02VW0EZ	Restriction of Thoracic Aorta, Descending with Branched or Fenestrated Intraluminal Device, One or Two Arteries, Open Approach
02VW0FZ	Restriction of Thoracic Aorta, Descending with Branched or Fenestrated Intraluminal Device, Three or More Arteries, Open Approach
02VW0ZZ	Restriction of Thoracic Aorta, Descending, Open Approach
02VW3EZ	Restriction of Thoracic Aorta, Descending with Branched or Fenestrated Intraluminal Device, One or Two Arteries, Percutaneous Approach
02VW3FZ	Restriction of Thoracic Aorta, Descending with Branched or Fenestrated Intraluminal Device, Three or More Arteries, Percutaneous Approach
02VW3ZZ	Restriction of Thoracic Aorta, Descending, Percutaneous Approach

ANY_REPAIR
defined as having ASC_REAPAIR, ARCH_REPAIR, DESC_REPAIR, or having any of the of the codes below:

38.35 Repair thoracic aorta
38.45 Resection thoracic aorta
39.73 TEVAR

Table S3: Description of chromatin marks from ENCODE.

Mark	ID	Description of source
DNase-seq	ENCSR422IIZ	Ascending aorta of 51year old female
DNase-seq	ENCSR968TPO	Ascending aorta of 53 year old female
ChIP-seq of H3k27ac	ENCSR318HUC	Thoracic aorta of 54 year old male
ChIP-seq of H3k27ac	ENCSR069UMW	Ascending aorta of 53 year old female

Table S4: Relationship of TAA index variant (rs4073288) with T2D independent variants in *TCF7L2* locus.

T2D independent variants	LD R^2 with rs4073288	TAA p-value of rs4073288 after conditioning with T2D variant
rs7903146	0.2846	4.5×10^{-4}
rs536643418	0.0073	2.4×10^{-8}
rs140242150	0.0008	3.5×10^{-8}
rs7918400	0.08	3.1×10^{-6}
rs184509201	0.0004	3.8×10^{-8}
rs180988137	0.0132	6.1×10^{-8}
rs78025551	0.2468	4.5×10^{-5}
rs34855922	0.0203	3.9×10^{-8}

Table S5: Description of RegulomeDB ranks and associated variant count in 95% credible set of *TCF7L2* locus.

RegulomeDB rank	Description	Variant count
3a	TF binding + any motif + DNase peak	2
4	TF binding + DNase peak	4
5	TF binding or DNase peak	12
6	Motif hit	5
7	Others	9

Table S6: Genetic correlation between TAA and other traits as measured by LDSC.

Trait	r_g	S.E.	P	Source/PMID
SBP	-0.0069	0.0813	0.9327	UKBB
DBP	0.2713	0.0916	0.0031	UKBB
Smoking Initiation	0.1966	0.1902	0.3011	30617275
Cig. Per day	0.211	0.1586	0.1833	30617275
Total cholesterol	0.0314	0.1286	0.8072	20686565
HDL	-0.0905	0.1336	0.4983	20686565
LDL	0.0271	0.1565	0.8623	20686565
Triglyceride	0.2149	0.1197	0.0725	20686565
CAD	0.1749	0.108	0.1054	26343387
T2D	0.006	0.147	0.963	22885922
Height	0.3286	0.1139	0.0039	20881960

Table S7: Primers used for qPCR.

Gene	Sequence: 5’ to 3’
BCL2	Forward:TCATGTGTGTGGAGAGCGTC
	Reverse:GCCGTACAGTTCCACAAAGG
BAX	Forward:CCCGAGAGGTCTTTTTCCGAG
	Reverse:CCAGCCCATGATGGTTCTGAT
TCF7L2	Forward:GAATCGTCCCAGAGTGATGTC
	Reverse:ACGACCTTTGCTCTCATTTCC
ACTB	Forward:GCTATCACCTCCCCTGTGTG
	Reverse:GTCATTCCAAATATGAGATGCGT

Table S8: Effect-size variation within discovery cohort.

TCF7L2 (rs7904519)							
	N_{case}	$N_{control}$	AF_{case}	$AF_{control}$	OR	95% CI	Chi-square P
$CHIP_{cases}/MGI_{controls}$	956	18295	0.414	0.473	0.78	0.71-0.86	3.6×10^{-7}
$MGI_{cases}/MGI_{controls}$	395	18295	0.434	0.473	0.84	0.73-0.97	0.02
$CHIP_{AA}/MGI_{controls}$	773	18295	0.416	0.473	0.79	0.71-0.87	9.7×10^{-6}
$CHIP_{DA}//MGI_{controls}$	83	18295	0.349	0.473	0.59	0.43-0.82	0.001
FBN1(rs16961065)							
	N_{case}	$N_{control}$	AF_{case}	$AF_{control}$	OR	95% CI	Chi-square P
$CHIP_{cases}/MGI_{controls}$	956	18295	0.142	0.10	1.48	1.29-1.69	4.1×10^{-9}
$MGI_{cases}/MGI_{controls}$	395	18295	0.124	0.10	1.27	1.02-1.57	0.02
$CHIP_{AA}/MGI_{controls}$	773	18295	0.142	0.10	1.48	1.27-1.71	1.1×10^{-7}
$CHIP_{DA}//MGI_{controls}$	83	18295	0.114	0.10	1.17	0.70-1.84	0.53

$CHIP_{AA}$: ascending thoracic aneurysm in CHIP; $CHIP_{DA}$: descending thoracic aneurysm in CHIP

Table S9: Effect-size variation by phenotype definition within MVP cohort.

	EA	TAA N_{case}=6554				Any Thoracic Aortic Repair N_{case}=730				Ascending + Arch Repair N_{case}=444			
		Beta	SE	OR 95% CI	P	Beta	SE	OR 95% CI	P	Beta	SE	OR 95% CI	P
rs4073288 (*TCF7L2*)	A	-0.06	0.02	0.90-0.98	3.6×10^{-3}	-0.11	0.06	0.8-1	0.05	-0.11	0.07	0.78-1.03	0.14
rs7904519 (*TCF7L2*)	G	-0.06	0.02	0.90-0.98	4×10^{-4}	-0.12	0.05	0.8-0.98	0.03	-0.13	0.07	0.76-1	0.06
rs4074718 (*TCF7L2*)	A	-0.06	0.02	0.90-0.98	8×10^{-4}	-0.15	0.06	0.76-0.97	9×10^{-3}	-0.15	0.07	0.75-0.99	0.04
Rs591519 (*FBN1*)	T	0.24	0.03	1.20-1.35	9×10^{-20}	0.48	0.07	1.41-1.85	1.4×10^{-10}	0.57	0.09	1.48-2.11	4.6×10^{-10}

$N_{control}$=329971 for all comparisons

VA Million Veteran Program: Core Acknowledgement for Publications
Updated December 10, 2020

MVP Executive Committee

- Co-Chair: J. Michael Gaziano, M.D., M.P.H.
  VA Boston Healthcare System, 150 S. Huntington Avenue, Boston, MA 02130
- Co-Chair: Sumitra Muralidhar, Ph.D.
  US Department of Veterans Affairs, 810 Vermont Avenue NW, Washington, DC 20420
- Rachel Ramoni, D.M.D., Sc.D., Chief VA Research and Development Officer
  US Department of Veterans Affairs, 810 Vermont Avenue NW, Washington, DC 20420
- Jean Beckham, Ph.D.
  Durham VA Medical Center, 508 Fulton Street, Durham, NC 27705
- Kyong-Mi Chang, M.D.
  Philadelphia VA Medical Center, 3900 Woodland Avenue, Philadelphia, PA 19104
- Christopher J. O'Donnell, M.D., M.P.H.
  VA Boston Healthcare System, 150 S. Huntington Avenue, Boston, MA 02130
- Philip S. Tsao, Ph.D.
  VA Palo Alto Health Care System, 3801 Miranda Avenue, Palo Alto, CA 94304
- James Breeling, M.D., Ex-Officio
  US Department of Veterans Affairs, 810 Vermont Avenue NW, Washington, DC 20420
- Grant Huang, Ph.D., Ex-Officio
  US Department of Veterans Affairs, 810 Vermont Avenue NW, Washington, DC 20420
- Juan P. Casas, M.D., Ph.D., Ex-Officio
  VA Boston Healthcare System, 150 S. Huntington Avenue, Boston, MA 02130

MVP Program Office

- Sumitra Muralidhar, Ph.D.
  US Department of Veterans Affairs, 810 Vermont Avenue NW, Washington, DC 20420
- Jennifer Moser, Ph.D.
  US Department of Veterans Affairs, 810 Vermont Avenue NW, Washington, DC 20420

MVP Recruitment/Enrollment

- Recruitment/Enrollment Director/Deputy Director, Boston – Stacey B. Whitbourne, Ph.D.; Jessica V. Brewer, M.P.H.
  VA Boston Healthcare System, 150 S. Huntington Avenue, Boston, MA 02130
- MVP Coordinating Centers
  - Clinical Epidemiology Research Center (CERC), West Haven – Mihaela Aslan, Ph.D.
    West Haven VA Medical Center, 950 Campbell Avenue, West Haven, CT 06516

    - Cooperative Studies Program Clinical Research Pharmacy Coordinating Center, Albuquerque – Todd Connor, Pharm.D.; Dean P. Argyres, B.S., M.S.
      New Mexico VA Health Care System, 1501 San Pedro Drive SE, Albuquerque, NM 87108
    - Genomics Coordinating Center, Palo Alto – Philip S. Tsao, Ph.D.
      VA Palo Alto Health Care System, 3801 Miranda Avenue, Palo Alto, CA 94304
    - MVP Boston Coordinating Center, Boston - J. Michael Gaziano, M.D., M.P.H.
      VA Boston Healthcare System, 150 S. Huntington Avenue, Boston, MA 02130
    - MVP Information Center, Canandaigua – Brady Stephens, M.S.
      Canandaigua VA Medical Center, 400 Fort Hill Avenue, Canandaigua, NY 14424
- VA Central Biorepository, Boston – Mary T. Brophy M.D., M.P.H.; Donald E. Humphries, Ph.D.; Luis E. Selva, Ph.D.
  VA Boston Healthcare System, 150 S. Huntington Avenue, Boston, MA 02130
- MVP Informatics, Boston – Nhan Do, M.D.; Shahpoor (Alex) Shayan, M.S.
  VA Boston Healthcare System, 150 S. Huntington Avenue, Boston, MA 02130
- MVP Data Operations/Analytics, Boston – Kelly Cho, M.P.H., Ph.D.
  VA Boston Healthcare System, 150 S. Huntington Avenue, Boston, MA 02130
- Director of Regulatory Affairs – Lori Churby, B.S.
  VA Palo Alto Health Care System, 3801 Miranda Avenue, Palo Alto, CA 94304

MVP Science

- Science Operations – Christopher J. O'Donnell, M.D., M.P.H.
  VA Boston Healthcare System, 150 S. Huntington Avenue, Boston, MA 02130
- Genomics Core – Christopher J. O'Donnell, M.D., M.P.H.; Saiju Pyarajan Ph.D.
  VA Boston Healthcare System, 150 S. Huntington Avenue, Boston, MA 02130
  Philip S. Tsao, Ph.D.
  VA Palo Alto Health Care System, 3801 Miranda Avenue, Palo Alto, CA 94304
- Data Core – Kelly Cho, M.P.H, Ph.D.
  VA Boston Healthcare System, 150 S. Huntington Avenue, Boston, MA 02130
- VA Informatics and Computing Infrastructure (VINCI) – Scott L. DuVall, Ph.D.
  VA Salt Lake City Health Care System, 500 Foothill Drive, Salt Lake City, UT 84148
- Data and Computational Sciences – Saiju Pyarajan, Ph.D.
  VA Boston Healthcare System, 150 S. Huntington Avenue, Boston, MA 02130
- Statistical Genetics – Elizabeth Hauser, Ph.D.
  Durham VA Medical Center, 508 Fulton Street, Durham, NC 27705
  Yan Sun, Ph.D.
  Atlanta VA Medical Center, 1670 Clairmont Road, Decatur, GA 30033
  Hongyu Zhao, Ph.D.
  West Haven VA Medical Center, 950 Campbell Avenue, West Haven, CT 06516

Current MVP Local Site Investigators

- Atlanta VA Medical Center (Peter Wilson, M.D.)
  1670 Clairmont Road, Decatur, GA 30033
- Bay Pines VA Healthcare System (Rachel McArdle, Ph.D.)
  10,000 Bay Pines Blvd Bay Pines, FL 33744
- Birmingham VA Medical Center (Louis Dellitalia, M.D.)
  700 S. 19th Street, Birmingham AL 35233
- Central Western Massachusetts Healthcare System (Kristin Mattocks, Ph.D., M.P.H.)
  421 North Main Street, Leeds, MA 01053
- Cincinnati VA Medical Center (John Harley, M.D., Ph.D.)
  3200 Vine Street, Cincinnati, OH 45220
- Clement J. Zablocki VA Medical Center (Jeffrey Whittle, M.D., M.P.H.)
  5000 West National Avenue, Milwaukee, WI 53295
- VA Northeast Ohio Healthcare System (Frank Jacono, M.D.)
  10701 East Boulevard, Cleveland, OH 44106
- Durham VA Medical Center (Jean Beckham, Ph.D.)
  508 Fulton Street, Durham, NC 27705
- Edith Nourse Rogers Memorial Veterans Hospital (John Wells., Ph.D.)
  200 Springs Road, Bedford, MA 01730
- Edward Hines, Jr. VA Medical Center (Salvador Gutierrez, M.D.)
  5000 South 5th Avenue, Hines, IL 60141
- Veterans Health Care System of the Ozarks (Gretchen Gibson, D.D.S., M.P.H.)
  1100 North College Avenue, Fayetteville, AR 72703
- Fargo VA Health Care System (Kimberly Hammer, Ph.D.)
  2101 N. Elm, Fargo, ND 58102
- VA Health Care Upstate New York (Laurence Kaminsky, Ph.D.)
  113 Holland Avenue, Albany, NY 12208
- New Mexico VA Health Care System (Gerardo Villareal, M.D.)
  1501 San Pedro Drive, S.E. Albuquerque, NM 87108
- VA Boston Healthcare System (Scott Kinlay, M.B.B.S., Ph.D.)
  150 S. Huntington Avenue, Boston, MA 02130
- VA Western New York Healthcare System (Junzhe Xu, M.D.)
  3495 Bailey Avenue, Buffalo, NY 14215-1199
- Ralph H. Johnson VA Medical Center (Mark Hamner, M.D.)
  109 Bee Street, Mental Health Research, Charleston, SC 29401
- Columbia VA Health Care System (Roy Mathew, M.D.)
  6439 Garners Ferry Road, Columbia, SC 29209
- VA North Texas Health Care System (Sujata Bhushan, M.D.)
  4500 S. Lancaster Road, Dallas, TX 75216
- Hampton VA Medical Center (Pran Iruvanti, D.O., Ph.D.)
  100 Emancipation Drive, Hampton, VA 23667

- Richmond VA Medical Center (Michael Godschalk, M.D.)
  1201 Broad Rock Blvd., Richmond, VA 23249
- Iowa City VA Health Care System (Zuhair Ballas, M.D.)
  601 Highway 6 West, Iowa City, IA 52246-2208
- Eastern Oklahoma VA Health Care System (Douglas Ivins, M.D.)
  1011 Honor Heights Drive, Muskogee, OK 74401
- James A. Haley Veterans' Hospital (Stephen Mastorides, M.D.)
  13000 Bruce B. Downs Blvd, Tampa, FL 33612
- James H. Quillen VA Medical Center (Jonathan Moorman, M.D., Ph.D.)
  Corner of Lamont & Veterans Way, Mountain Home, TN 37684
- John D. Dingell VA Medical Center (Saib Gappy, M.D.)
  4646 John R Street, Detroit, MI 48201
- Louisville VA Medical Center (Jon Klein, M.D., Ph.D.)
  800 Zorn Avenue, Louisville, KY 40206
- Manchester VA Medical Center (Nora Ratcliffe, M.D.)
  718 Smyth Road, Manchester, NH 03104
- Miami VA Health Care System (Hermes Florez, M.D., Ph.D.)
  1201 NW 16th Street, 11 GRC, Miami FL 33125
- Michael E. DeBakey VA Medical Center (Olaoluwa Okusaga, M.D.)
  2002 Holcombe Blvd, Houston, TX 77030
- Minneapolis VA Health Care System (Maureen Murdoch, M.D., M.P.H.)
  One Veterans Drive, Minneapolis, MN 55417
- N. FL/S. GA Veterans Health System (Peruvemba Sriram, M.D.)
  1601 SW Archer Road, Gainesville, FL 32608
- Northport VA Medical Center (Shing Shing Yeh, Ph.D., M.D.)
  79 Middleville Road, Northport, NY 11768
- Overton Brooks VA Medical Center (Neeraj Tandon, M.D.)
  510 East Stoner Ave, Shreveport, LA 71101
- Philadelphia VA Medical Center (Darshana Jhala, M.D.)
  3900 Woodland Avenue, Philadelphia, PA 19104
- Phoenix VA Health Care System (Samuel Aguayo, M.D.)
  650 E. Indian School Road, Phoenix, AZ 85012
- Portland VA Medical Center (David Cohen, M.D.)
  3710 SW U.S. Veterans Hospital Road, Portland, OR 97239
- Providence VA Medical Center (Satish Sharma, M.D.)
  830 Chalkstone Avenue, Providence, RI 02908
- Richard Roudebush VA Medical Center (Suthat Liangpunsakul, M.D., M.P.H.)
  1481 West 10th Street, Indianapolis, IN 46202
- Salem VA Medical Center (Kris Ann Oursler, M.D.)
  1970 Roanoke Blvd, Salem, VA 24153

- San Francisco VA Health Care System (Mary Whooley, M.D.)
  4150 Clement Street, San Francisco, CA 94121
- South Texas Veterans Health Care System (Sunil Ahuja, M.D.)
  7400 Merton Minter Boulevard, San Antonio, TX 78229
- Southeast Louisiana Veterans Health Care System (Joseph Constans, Ph.D.)
  2400 Canal Street, New Orleans, LA 70119
- Southern Arizona VA Health Care System (Paul Meyer, M.D., Ph.D.)
  3601 S 6th Avenue, Tucson, AZ 85723
- Sioux Falls VA Health Care System (Jennifer Greco, M.D.)
  2501 W 22nd Street, Sioux Falls, SD 57105
- St. Louis VA Health Care System (Michael Rauchman, M.D.)
  915 North Grand Blvd, St. Louis, MO 63106
- Syracuse VA Medical Center (Richard Servatius, Ph.D.)
  800 Irving Avenue, Syracuse, NY 13210
- VA Eastern Kansas Health Care System (Melinda Gaddy, Ph.D.)
  4101 S 4th Street Trafficway, Leavenworth, KS 66048
- VA Greater Los Angeles Health Care System (Agnes Wallbom, M.D., M.S.)
  11301 Wilshire Blvd, Los Angeles, CA 90073
- VA Long Beach Healthcare System (Timothy Morgan, M.D.)
  5901 East 7th Street Long Beach, CA 90822
- VA Maine Healthcare System (Todd Stapley, D.O.)
  1 VA Center, Augusta, ME 04330
- VA New York Harbor Healthcare System (Scott Sherman, M.D., M.P.H.)
  423 East 23rd Street, New York, NY 10010
- VA Pacific Islands Health Care System (George Ross, M.D.)
  459 Patterson Rd, Honolulu, HI 96819
- VA Palo Alto Health Care System (Philip Tsao, Ph.D.)
  3801 Miranda Avenue, Palo Alto, CA 94304-1290
- VA Pittsburgh Health Care System (Patrick Strollo, Jr., M.D.)
  University Drive, Pittsburgh, PA 15240
- VA Puget Sound Health Care System (Edward Boyko, M.D.)
  1660 S. Columbian Way, Seattle, WA 98108-1597
- VA Salt Lake City Health Care System (Laurence Meyer, M.D., Ph.D.)
  500 Foothill Drive, Salt Lake City, UT 84148
- VA San Diego Healthcare System (Samir Gupta, M.D., M.S.C.S.)
  3350 La Jolla Village Drive, San Diego, CA 92161
- VA Sierra Nevada Health Care System (Mostaqul Huq, Pharm.D., Ph.D.)
  975 Kirman Avenue, Reno, NV 89502
- VA Southern Nevada Healthcare System (Joseph Fayad, M.D.)
  6900 North Pecos Road, North Las Vegas, NV 89086

- VA Tennessee Valley Healthcare System (Adriana Hung, M.D., M.P.H.)
  1310 24th Avenue, South Nashville, TN 37212
- Washington DC VA Medical Center (Jack Lichy, M.D., Ph.D.)
  50 Irving St, Washington, D. C. 20422
- W.G. (Bill) Hefner VA Medical Center (Robin Hurley, M.D.)
  1601 Brenner Ave, Salisbury, NC 28144
- White River Junction VA Medical Center (Brooks Robey, M.D.)
  163 Veterans Drive, White River Junction, VT 05009
- William S. Middleton Memorial Veterans Hospital (Robert Striker, M.D., Ph.D.)
  2500 Overlook Terrace, Madison, WI 53705